

Photocatalytic Degradation of Methylene Blue by Tin and Indium doped Sol-Gel Reflux Synthesized Titania



By

Junaid ur Rehman

School of Chemical and Materials Engineering (SCME)

**National University of Sciences and Technology
(NUST)**

2017

Photocatalytic Degradation of Methylene Blue by Tin and Indium doped Sol-Gel Reflux Synthesized Titania



Junaid ur Rehman

00000119710

This thesis is submitted as a partial fulfillment of the requirements for the
degree of Master of Science in Materials & Surface Engineering

MS in Materials & Surface Engineering

Supervisor: Dr. Sofia Javed

School of Chemical and Materials Engineering (SCME)

National University of Sciences and Technology (NUST), H-12

Islamabad, Pakistan

June, 2017

Certificate

This is to certify that work in this thesis has been carried out by **Mr. Junaid ur Rehman** and completed under my supervision in nano laboratory, School of Chemical and Materials Engineering, National University of Sciences and Technology, H-12, Islamabad, Pakistan.

Supervisor: _____

Co-supervisor _____
Mujahid

Prof. Dr. Mohammad

Submitted through

Principal/Dean

Materials Engineering Department

National University of Sciences and Technology, Islamabad

I would like to dedicate this thesis to my beloved parents, siblings and affectionate teachers

Acknowledgement

I am pleased to express my appreciation to all those who supported me in making this thesis a reality. I express my profound sense of respect to my supervisor Dr. Sofia Javed who gave me the opportunity to work on this project. Her continuous support, motivation and tireless guidance have resulted in successful completion of this project. Her vast knowledge, calm nature and positive criticism motivated me to strive to nice results. Thanks to her for tolerating my mistakes. I would also like to pay my humble gratitude to Dr. Mohammad Mujahid and Dr. Aftab Akram for throughout helping and guiding me whenever I needed some. I would like to acknowledge the timely help when needed from my research fellows Mr. Hafiz Fayzan Shakkir and Ms. Ramsha Khan. Also, I would like to thank IESE, NUST and CIIT, Islamabad for letting me do UV-Vis spectroscopy and Raman spectroscopy respectively.

Last but not the least, I would like to thank my kind parents and siblings for their constant support, prayers and best wishes. They enriched my morale whenever I needed it.

Junaid ur Rehman, June 2017

Abstract

Photocatalytic Degradation of Methylene Blue by Tin and Indium doped Sol-Gel Reflux Synthesized Titania

Titania has been most widely used for photocatalytic degradation study of organic pollutants due to its cost effectiveness, inert nature and photo-stability. Titanium dioxide (TiO_2) powder was synthesized via sol-gel refluxing using titanium tetraisopropoxide (TTIP) as precursor. TiO_2 powder was doped with varying concentrations of tin and indium. Scanning Electron Microscopy (SEM) and Atomic Force Microscopy (AFM) analysis revealed the particle size between 12-22nm. X-ray diffraction (XRD) and Raman confirmed the formation of phase pure nanocrystalline anatase. Fourier transform infrared spectroscopy (FTIR) confirmed the presence of Ti-O-Ti bonding. Surface area analysis was done via Brunauer Emett Teller (BET) analysis. Finally UV-Vis spectroscopy was used for optical characterizations. Photocatalytic decomposition of methylene blue was investigated under ultraviolet irradiation for 8 hours. The higher photocatalytic decomposition of methylene blue solution was achieved with Tin doped titania than indium doped or pure titania.

Table of Content

Certificate.....	i
Dedication.....	ii
Acknowledgement	iii
Abstract.....	iv
Table of Content.....	v
List of Figures.....	viii
List of Tables.....	xi

Chapter 1

1.1 Background of study	1
1.2 Literature Review.....	1
1.2.1 TiO ₂ and its applications.....	2
1.2.2 Basic Principle of Photocatalysis.....	2
1.2.3 Mechanism of TiO ₂ Photocatalysis.....	3
1.2.4 Titania and the various existing photocatalyst	4
1.2.5 Titania as photocatalyst and existing challenges	6
1.2.6 Drawbacks and attempts to improve photocatalytic activity of TiO ₂	6
1.2.6.1 Modification and novel titania photocatalyst preparations.....	6
1.2.7 Effects of synthesis route for photocatalyst	8
1.2.8 Methods for titania photocatalyst synthesis.....	9
1.2.8.1 Sol-gel method.....	9
1.2.8.2 Advantages of sol-gel synthesis.....	9
1.2.8.3 What is sol-gel process?	10
1.2.8.4 Challenges and Solutions.....	10
1.3 Objectives	10

Chapter 2

Materials Selection and Procurement

2.1 Materials and Methods.....	12
2.2 Chemicals Required	12
2.3 Experimentation.....	13

2.3.1 Safety Precautions.....	13
2.3.2 Calculations.....	13
2.3.3 Synthesis of Titania Nanoparticles.....	14
2.3.3.1 Sol-gel synthesis.....	14
2.3.3.2 Refluxing.....	15
2.3.3.3 Drying.....	15
2.3.3.4 Pestle and Mortar.....	15
2.3.3.5 Annealing.....	16

Chapter 3

Characterizations

3.1 XRD Analysis.....	18
3.2 Scanning Electron Microscopy.....	19
3.3 FTIR.....	20
3.4 UV-Vis Spectroscopy.....	21
3.5 AFM.....	22
3.6 BET.....	22
3.7 Raman Spectroscopy.....	23
3.8 Photocatalytic Degradation.....	24

Chapter 4

Results and Discussions

4.1 Synthesis of Titania Nanoparticles.....	25
4.1.1 Mechanism of Sol-gel Synthesis.....	25
4.1.1.1 Acetic Acid Modification of TTIP.....	25
4.2 SEM.....	26
4.3 BET.....	29
4.4 AFM.....	30
4.5 XRD.....	33
4.6 Raman Spectroscopy.....	34
4.7 UV-Vis Spectroscopy.....	35
4.8 FTIR.....	39

4.9 Photocatalytic Degradation.....	41
Chapter 5	
5.1 Conclusions.....	44
5.2 Future Recommendations.....	45
References.....	46

List of Figures

1.1	Photophysical and photochemical processes when photon activates semiconductor cluster (p) electron/hole pair generation, (q) recombination on surface, (r) bulk recombination, (s) acceptor and reduction diffusion on SC surface, and (t) donor oxidation on SC particle surface.....	3
1.2	Conduction and valence band positions of various metal oxide semiconductors. Left hand scale is for the internal energies with respect to vacuum level while the right hand scale is for normal hydrogen electrode which allows oxidation & reduction based predictions.....	5
1.3	Metal doped titania photocatalyst modification.....	7
1.4	Band diagram for transferring charge carrier in coupled semiconductor.....	9
2.1	Flow Sheet for titania nanoparticles synthesis.....	16
2.2	Mixing of precursor and chelating agent.....	17
2.3	Hydrolysis.....	17
2.4	Sol-gel after refluxing.....	17
2.5	Titania nano powder after drying, grinding and annaealing.....	17
3.1	XRD instrument.....	18
3.2	SEM equipment.....	19
3.3	Hydraulic Press for making FTIR Billets.....	20
3.4	FTIR instrumentation.....	21
3.5	UV-Vis instrumentation.....	21
3.6	AFM instrument.....	22
3.7	BET surface area analyzer.....	23
3.8	Raman Spectroscopy instrumentation.....	23
3.9	Photocatalysis Chamber available in IESE.....	24
3.10	UV-lamp chamber.....	24
4.1	SEM image for pure titania.....	27
4.2	SEM image for 0.25% Sn doped titania.....	27

4.3	SEM image for 0.50% Sn doped titania.....	27
4.4	SEM image for 0.75% Sn doped titania.....	27
4.5	SEM image for 0.25% In doped titania.....	27
4.6	SEM image for 0.50% In doped titania.....	27
4.7	SEM image for 0.75% In doped titania.....	28
4.8	Topography for sol-gel reflux synthesized pure titania.....	30
4.9	Topography for 0.25% Sn doped sol-gel reflux synthesized titania.....	30
4.10	Topography for 0.50% Sn doped sol-gel reflux synthesized titania.....	31
4.11	Topography for 0.75% Sn doped sol-gel reflux synthesized titania.....	31
4.12	Topography for 0.25% In doped sol-gel reflux synthesized titania.....	31
4.13	Topography for 0.50% In doped sol-gel reflux synthesized titania.....	31
4.14	Topography for 0.75% In doped sol-gel reflux synthesized titania.....	32
4.15	XRD plot for doped and un-doped titania.....	33
4.16	Raman shifts for doped and un-doped titania.....	35
4.17	UV-Vis absorption spectrum for doped and un-doped titania.....	36
4.18	UV-Vis transmittance spectrum for doped and un-doped titania.....	36
4.19	Tauc's plot for sol-gel reflux synthesized pure titania.....	37
4.20	Tauc's plot for 0.25% Sn doped titania.....	38
4.21	Tauc's plot for 0.50% Sn doped titania.....	38
4.22	Tauc's plot for 0.75% Sn doped titania.....	38
4.23	Tauc's plot for 0.25% In doped titania.....	38
4.24	Tauc's plot for 0.50% In doped titania.....	38
4.25	Tauc's plot for 0.75% In doped titania.....	38
4.26	FTIR plot for doped and un-doped titania.....	40
4.27	Photocatalysis degradation of methylene blue by Tin doped titania.....	41
4.28	Photocatalysis degradation of methylene blue by Indium doped titania.....	42

4.29	Change in color & concentration of MB with time.....	42
------	--	----

List of Tables

2.1	Chemicals used and their respective roles.....	12
2.2	Calculation for dopant wt%.....	14
2.3	Various sol-gel samples with varying type and amount of doping.....	15
4.1	Description of samples.....	26
4.2	Particles size as revealed by SEM.....	28
4.3	BET surface area values.....	29
4.4	Particle size for doped and undoped titania as by AFM.....	32
4.5	Crystallite size of doped and un-doped titania as by XRD.....	34
4.6	Band gap values by Tauc's plot for doped and un-doped titania samples.....	39
4.7	Wavenumbers of FTIR peaks	40

Chapter-1

Introduction

1.1 Background of study

Due to increase in organic and inorganic pollutants in air and wastewater streams, the laws for environment have been becoming stricter [1,2]. There is therefore urgency for establishment of eco-friendly systems to counter these pollutants.

Both atmospheric organic and aquatic contaminants have been effectively treated by heterogeneous photocatalysis [3]. Heterogeneous photocatalysis is acceleration via photoreaction when some semiconductor photocatalyst is available. Photocatalytic oxidation (PCO) is one of the major applications of heterogeneous catalysis for effective partial or complete mineralization of contaminants [4]. Degradation starts with a partial degradation, the term ‘photocatalytic degradation’ however refers to complete photocatalytic oxidation, essentially to CO_2 , H_2O , NO_3^- , PO_4^{3-} and halide ions [5].

Titania photocatalysis or “Honda–Fujishima effect” was the fruit of research by Fujishima and Honda [6]. They found out the probability of splitting water by photoelectrochemical cell provided with an inert cathode and rutile titania anode. As a result, titania photocatalysis found its excess to environmental frontiers.

Heterogeneous photocatalysis has been a field of constant focus since its discovery and various books and research have been done on it [5,7]. Although there are many applications of photocatalysis but the basic photophysical principle and physical chemistry usually remains the same. Photocatalytic degradation has wide range of destruction for both organic and inorganic contaminants. The detailed principle of photocatalytic degradation is discussed in the following.

1.2 Literature Review

Vast research has been done in the past about 40 odd years for the growth of heterogeneous photocatalytic technology to remove organic and inorganic pollutants [8-15]. Semiconductors with suitable band gap have been usually used as the photocatalysts, such as TiO_2 , ZnO , Fe_2O_3 , CdS , ZnS , and ZrO_2 .

1.2.1 TiO₂ and its applications

Owing to its incredible potential to be used as photocatalyst because of its properties like suitable flat band potential, chemically stable, non-toxic and high Photocatalytic activity titania (TiO₂) have been the most commonly used semiconductor [11,16-21]. TiO₂ is been widely used in our daily lives like in cosmetics, paints and food color etc. TiO₂ is based on light-induced catalysis oxidizing and reducing reactions on semiconductor surface owing to its photo catalytic properties. It was initially not fully understood and 'chalking', the photo-activity of TiO₂ was seen as a considerable problem that affected the durability of TiO₂-based paints. That is, like a chalk on a blackboard the organic components of TiO₂-containing paints are partially decomposed and white powdery TiO₂ is exposed on the surface when exposed to strong sunlight [22,23]. Since the discovery of photocatalytic splitting of water molecules by Fujishima and Honda [22-24], various photo catalytic properties of TiO₂ [25,26], applications as water conversion to hydrogen and oxygen [24, 27], CO₂ conversion to hydrocarbons [28,29], disinfection of water and air [30-32], self-cleaning surfaces [33], and antimicrobial biomedical materials [34] have been under focus.

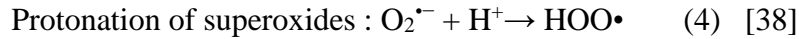
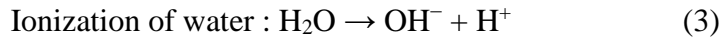
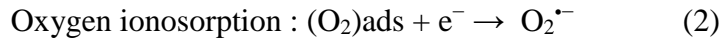
1.2.2 Basic Principle of Photocatalysis

Heterogeneous photocatalysis include many reactions as water splitting, organic synthesis, hydrogen transfer, photo-reduction, and disinfection. [5,35]. However titania assisted heterogeneous photocatalytic oxidation has been used for years as method for purification of air and water streams.

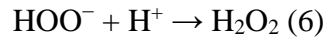
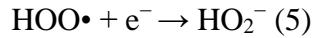
Basic photophysical and photochemical principles of photocatalysis have already been reported in literatures [36,37]. It has been reported that the molecules that are in direct contact with the catalyst surface undergo photocatalytic degradation [38].

In photocatalysis reaction, a photon carrying energy $h\nu$ higher than the bandgap of semiconductor cause the excitation of electron from the filled valence band to the conduction band and thus creating hole in valence band while electron availability in conduction band. In this way electron-hole pair is created. Following reactions explain it more;





The hydroperoxyl radical formed in (4) also has scavenging property as O_2 thus doubly prolonging the lifetime of photohole:



Photooxidation and photoreduction can both take place at surface of the photo excited semiconductor photocatalyst (Fig. 1.1). Electron and hole recombine unless oxygen takes the electrons to form superoxides ($\text{O}_2^{\bullet-}$), its protonated form the hydroperoxyl radical (HO_2^{\bullet}) and subsequently H_2O_2 .

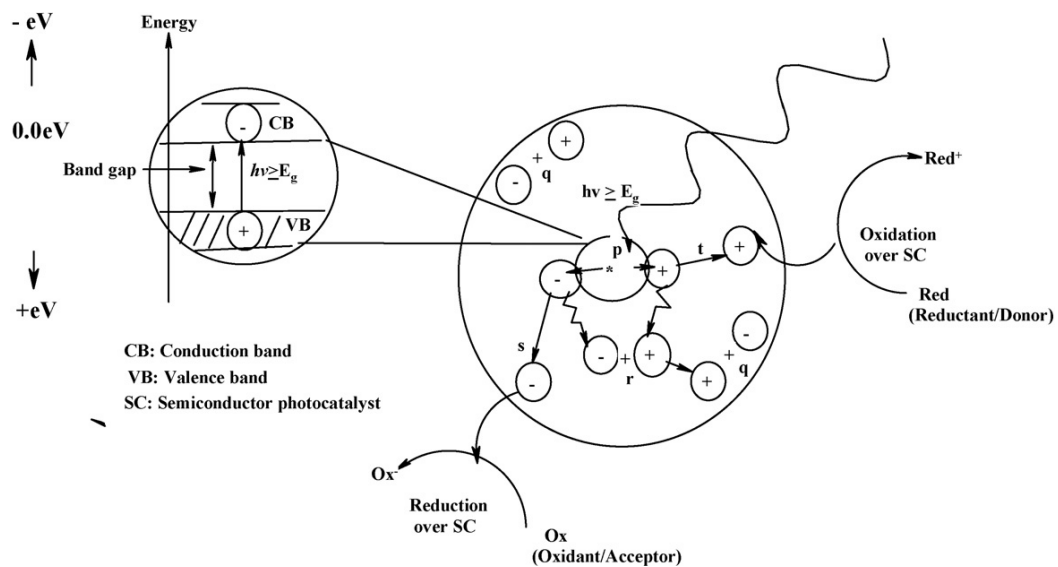


Fig.1.1. Photophysical and photochemical processes when photon activates semiconductor cluster (p) electron/hole pair generation, (q) recombination on surface, (r) bulk recombination, (s) acceptor and reduction diffusion on SC surface, and (t) donor oxidation on SC particle surface. [38]

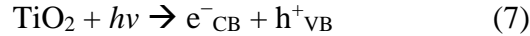
1.2.3 Mechanism of TiO_2 Photocatalysis

Mechanism of TiO_2 photo catalysis is based on electron-hole pair generation in a crystalline form of TiO_2 . Three of the many TiO_2 crystalline forms are:

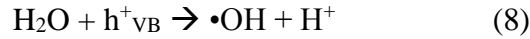
- anatase,
- brookite and,

- rutile

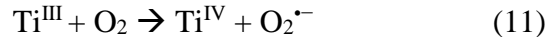
Anatase has band gap of 3.2 eV. As explained earlier in previous section when light of equal or greater energy (i.e. a wavelength less than approximately 385nm) irradiates it, free electrons (e^-_{CB}) and positively charged holes (h^+_{VB}), having strong reducing and oxidizing potentials, are created (Equation 7).



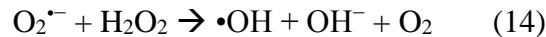
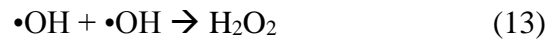
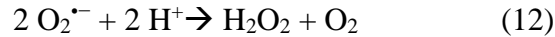
Recombination of electron-hole may occur at this point, however, catalyst surface adsorbed oxygen or water results in various oxidation or reduction reactions provided that electrons and/or holes move to the surface of the crystal [39]. Hydroxyl radicals ($\bullet\text{OH}$) are formed by water molecules trapped in the holes (Equations 8 and 9).



Ti^{IV} sites on TiO_2 surface may trap the conduction band electrons which reduce them to Ti^{III} sites. Oxygen on surface then react with Ti^{III} sites and generate superoxide radicals ($\text{O}_2^{\bullet-}$) (Equations 10 and 11) [40].



Formation of hydrogen peroxide (H_2O_2) or hydroperoxyl radicals ($\bullet\text{OOH}$) is lead by following reactions (Equations 12-15) [41].



$\bullet\text{OH}$, $\text{O}_2^{\bullet-}$, and H_2O_2 are considered as the key reactive oxygen species (ROS) in photo catalytic reaction, according to the literature [42]

1.2.4 Titania and the various existing photocatalysts

Photocatalytic oxidation is characterized ideal when it has following attributes [5]:

- (1) Photo-stability.
- (2) Chemical and biological inertness
- (3) Availability

(4) Low Cost

Many chalcogenide semiconductors like TiO_2 , ZnO , ZrO_2 , CdS , MoS_2 , Fe_2O_3 and WO_3 have been reserached as photocatalysts for the degrading organic contaminants [43]. Photo generation of charge carriers over TiO_2 semiconductor (anatase form) is occurred when the minimum band gap energy of photon is 3.2 eV (388nm) [44]. Photo activation for titania takes place in the range of 300–388 nm. Band-edge position of the semiconductor and the redox potentials of the adsorbates is the key for inducing electrons transfer [45]. For the research over two decades in a search for an ideal photocatalyst, anatase titania is still dealt as a standard for comparison to new entrants [46]. Anatase has been reported as phase of titania to have better photostability and Photocatalytic activity [4]. Almost all the studies have been done with crystalline form of anatase phase titania while a very few with amorphous having a significant amount of Photocatalytic activity [47]. Band positions for numerous semiconductors have been shown in Fig. 1.2.

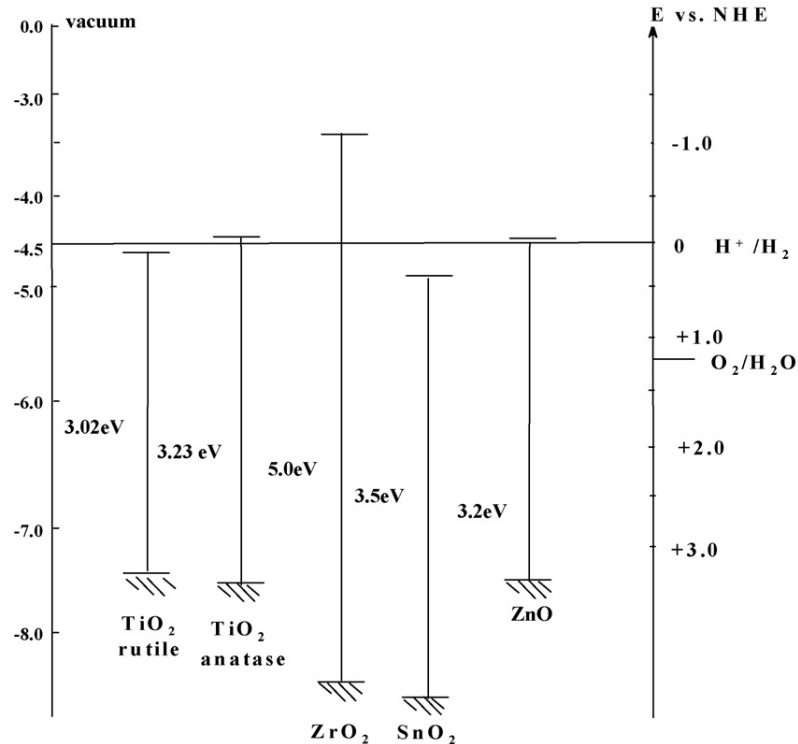


Fig.1.2. Conduction and valence band positions of various metal oxide semiconductors. Left hand scale is for the internal energies with respect to vacuum level while the right hand scale is for normal hydrogen electrode which allows oxidation & reduction based predictions.

1.2.5 Titania as photocatalyst and existing challenges

Titania as photocatalyst can be utilized in various forms as an independent free standing particulate, as a coating or as in most experiments it is used as powder particles suspended in contaminated water providing large surface area for photocatalytic activity [48]. Larger particulates may be useful but are commercially unavailable and costly [4]. Coated catalyst configurations though eliminate the need for catalyst filtration and centrifugation but results in reduction of system efficiency. A reduction upto 60-70% in performance is reported for aqueous systems of immobilized TiO₂ than to unsupported catalyst [49].

TiO₂ photocatalyst supports like soda lime glass, aluminium, ceramic tiles and coated glass have been reported [50-53]. Actual active surface area of photoreactor available compared to the overall volume is low as coatings are very thin. Even after all these mentioned drawbacks, coated photocatalysts and immobilisation techniques are still being investigated [54].

Titania has been used as photocatalyst for past decades owing to its potential for countering environmental pollution [55-57]. But titania is sensitive to only UV light as it has large band gap of 3.2eV, so that low efficiency is attained by solar light [58,59].

1.2.6 Drawbacks and Attempts to improve photocatalytic activity of TiO₂

Even after all drawbacks of using TiO₂ as photocatalyst many organic compounds /contaminants e.g endocrine disrupting compounds (EDCs) etc have been studied just with a point of view of water and air purification [60]. The basic exploration is to find a way to suppress electron-hole pair recombination and thus enhance the titania photosensitivity to apply it in applications [61].

1.2.6.1 Modification and novel titania photocatalyst preparations

Various attempts have been made to make titania a visible light sensitive by techniques like surface modification[62,63], metal or nonmetal ion doping [64-68], generating oxygen vacancy [69,70], combination with other semiconductors [71,72] etc. Doping with metals is categorized as second generation photocatalyst [57]. Doping titania with Fe³⁺, Mo⁵⁺, Ru³⁺, Os³⁺, Re⁵⁺, V⁴⁺, and Rh³⁺ at the 0.1-0.5% level enhanced

photocatalytic activity significantly, while Co^{3+} and Al^{3+} doping decreased photocatalytic activity [55,73]. According to Nagaveni work metal ion substituted titania has better Photocatalytic activity than commercial titania (Degussa P25) for photodegrading 4-nitrophenol [74].

To ensure effective photo activation there has been a constant growing need to go beyond 388nm the threshold wavelength corresponding to the titania band gap. For this the main focus was on following activities [75,76];

- incorporating energy levels into band gap of titania,
- changing life time of the charge carriers,
- substituting Ti^{4+} with cations having same size and
- enabling photoexcitation at lower energies by shifting conduction or valence band, which depends on method of preparation.

Above mentioned features have been tried to acquire via modification of the catalyst by doping, surface sensitization, coating with metal, enhancing surface area or by designing secondary titania photocatalyst. Recently increase in photocatalytic degradation of organic gaseous contaminants such as acetaldehyde and phenol over fluorinated titania surface have been observed. Reaction condition and the substrate kind effects the surface fluorination in a positive or negative manner [77].

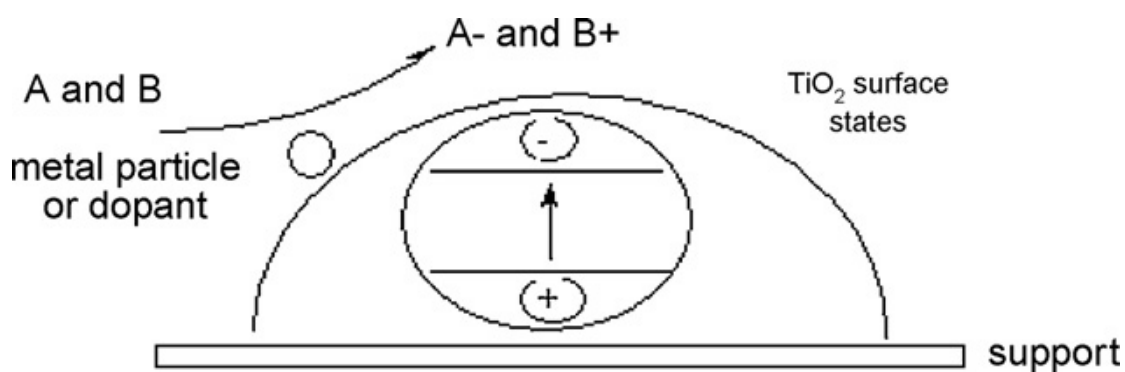


Fig.1.3. Metal doped titania photocatalyst modification

Since 1980s titania is modified mainly by metal to improve Photocatalytic activity [78-80]. Doping with transition metals to enhance its photocatalytic efficiency have also been reported (Fig. 1.3). Pt [81], N [82] and Fe [83,84] doping for titania and Zr have also been investigated. Though photophysical mechanism is not fully understood yet but

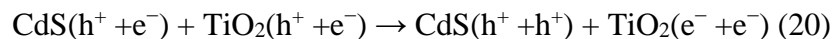
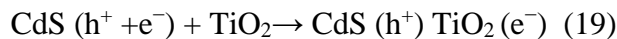
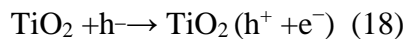
p-type metal ion dopants (with valencies $< \text{Ti}^{4+}$) are believed to act as acceptor centres opposite to the p-type [5]. Large shift of absorption band towards visible region is observed by metal ion implantation of TiO_2 e.g by Cr, Mn, V and Ni [5]. However there is no red shift in case of Ar and Ti implantation [85] of titania, indicating that bathochromic shift is not due to implantation itself.

Titania unlike other photocatalysts can absorb UV-A light in sun or room light form to improve its absorption beyond 388nm. Emphasis on visible light utilization for photoinduced process by Nozik is as old as photocatalysis itself. Abundant research have been devoted to the investigation of titania Photocatalytic oxidation [86,87], resulting in various visible responding metal or non-metal doped photocatalysts.

In this work, titania have been metal doped with Sn and In to see the effect of metal doping on bandgap of titania and its consequent effect on photocatalysis degradation of methylene blue.

1.2.7 Effects of synthesis route for photocatalyst

Procedure for photocatalyst synthesis has great effect on its catalytic activity especially for hybrid photocatalyst e.g $\text{TiO}_2\text{-SiO}_2$ [88,89], they have potential for removing VOCs [90]. While for $\text{TiO}_2\text{-ZrO}_2$ and $\text{TiO}_2\text{-SiO}_2$ hybrid oxides Photocatalytic activity is affected by crystalline structure, as recombination of electron-hole pair increase by crystallite defects [91]. Photocatalytic performance in 2-chlorophenol degradation with suspension of CdS and TiO_2 has been attained as reported by Doong et al. [92]. Inter-particle electron transfer (IPET) occur as shown by following processes (Fig. 1.4). IPET has been used widely to explain promotional effects in same kind of photocatalysis [93].



Electrons which are in excess on titania are taken by chemisorbed O_2 [94].

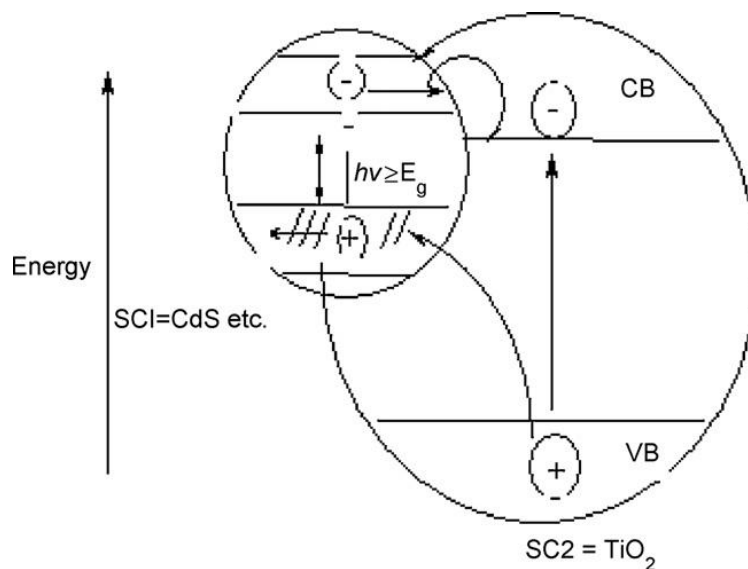


Fig1.4 Band diagram for transferring charge carrier in coupled semiconductor.

1.2.8 Methods for titania photocatalyst synthesis

Titania have been used for many commercial environmental applications like self-cleaning, anti – microbial activities and waste water purification [95]. Keeping ease of production and productivity in perspective TiO_2 have been synthesized by various techniques like flame synthesis, chemical vapor deposition and precipitation [96-98]. Sol-gel however is the most utilized technique for synthesizing titania photocatalyst.

1.2.8.1 Sol-gel method

Sol-gel processes [99] surpass other techniques for either growing titania films [100] or using it as powder [101].

1.2.8.2 Advantages of sol-gel synthesis

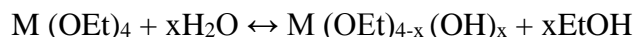
Pure and low cost products are resulted in by sol-gel due to simple processing route and high purity products availability. High crystal quality is achieved for titania during the sol-gel processing. Sol-gel is an attractive method for titania production as it allows tailoring structural properties like grain size, compositional homogeneity, porosity and particle morphology in solution phase, as it is carried out in solution [102]. High

reliability is ensured by optimal grain size growth and micro structure, by having uniform particle distribution [103,104].

1.2.8.3 What is Sol-gel process ?

In materials science, the sol-gel process is a method for producing solid materials from small molecules. The method is used for the fabrication of metal oxides, especially the oxides of silicon and titanium. The process involves conversion of monomers into a colloidal solution (sol) that acts as the precursor for an integrated network (or gel) of either discrete particles or network polymers. Typical sol-gel comprise of two steps; hydrolysis and condensation of precursors. Precursors are either metal alkoxides or inorganic and organic salts [99-101].

Hydrolysis:



Condensation:



1.2.8.4 Challenges and Solutions

In alkoxide sol-gel process alkoxide has tendency of taking up water molecules thus denting full outcome of sol-gel process. Use of modifiers like acetic acid and acetylene acetone ensure full outcome of sol-gel by altering ligand structure and thus avoiding water take up by alkoxide [105,106]. They control the hydrolysis and polycondensation reactions of sol-gel processing.

1.3 Objectives

The ultimate objective of this project was to synthesize the low cost and reproducible quality products for treating organic and inorganic pollutants. Studies were mostly done within the facilities of NUST.

The main objectives of this thesis work were;

- Synthesis of metal doped nanocrystalline titania powder via low cost solution based routes
- Morphological, phase, surface area, optical & functional group analysis for photocatalytic degradation studies
- To extend absorption range of titania towards visible wavelength and to reduce the bangap of titania
- Finally, to find out trends of Photocatalytic activity of doped and un-doped titania powders for photocatalysis degradation of methylene blue

Chapter-2

Material Selection & Procurement

2.1 Materials and Methods

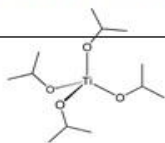
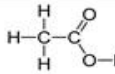
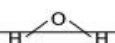
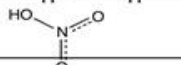
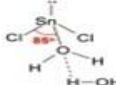

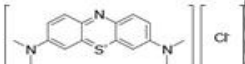
The present piece of research was done with a desire to move towards synthesizing the low cost, reproducible and highly efficient metal doped nanocrystalline photocatalyst to eliminate organic and inorganic contaminants. Following are the main aspects over which experimentation was done.

- Synthesis of doped and un-doped titania sol-gel
- Utilizing methylene blue as model pollutant for degradation studies
- Finding Photocatalytic activities and its trends for doped and undoped samples

2.2 Chemicals Required

In experimentation for this project following chemicals have been employed as mentioned in Table 2. TTIP was utilized as precursor, acetic acid as modifier, HNO₃ was used to facilitate peptization. Tin (II) chloride dehydrate and Indium (III) nitrate hydrate were the two salts used to have Sn and In doping respectively.

Table. 2.1. Chemicals used and their respective roles

Sr. No.	Chemical Name	Role to play	Chemical Formulae	Chemical Structure
1.	Titanium tetraisopropoxide (TTIP)	Precursor	Ti{OCH(CH ₃) ₂ } ₄	
2.	Acetic Acid	Modifier	CH ₃ COOH	
3.	Distilled Water	Hydrolysis	H ₂ O	
4.	Nitric Acid	Peptization	HNO ₃	
5.	Tin(II) Chloride Dihydrate	Sn Doping	SnCl ₂ . 2H ₂ O	
6.	Indium(III) nitrate hydrate	In Doping	In (NO ₃) ₃ . xH ₂ O	
7.	Methylene Blue	Dye	C ₁₆ H ₁₈ ClN ₃ S	

2.3 Experimentation

- Analytical grade chemicals were utilized
- The chemicals put to work as obtained with no more purification

2.3.1 Safety Precautions

Following precautions were ensured (Fig.2.9);

- Washed and dried all equipment properly
- Labeled every beaker, heating plate, round bottom flask, vials and petri-dish
- Used gloves and mask while handling the chemicals
- Switched off appliances when not being used
- Kept safe distance to avoid any inhaling of fumes
- Kept proper safety while working with UV-lamp for photocatalysis studies

2.3.2 Calculations

Actual moles (n_a) of titania in TTIP

11.4g of TTIP

No. of moles (n) = mass (m) / molar mass (mm)

$$n = 11.4\text{g} / 284.215\text{g}$$

$$n = 0.04 \text{ moles of TTIP}$$

mass of Titania (m) = 0.04 moles * 80g

$$m = 3.2\text{g of TiO}_2$$

% yield = actual yield / theoretical yield

$$12.5\% = \text{actual} / 3.2\text{g}$$

$$\text{actual} = 0.4\text{g of TiO}_2$$

$$\text{moles of TiO}_2 = 0.005 \text{ moles [} \frac{0.4}{80} \text{]}$$

Table.2.2. Calculations for dopant wt%

Dopant Type	wt%	No.of dopant moles (no. of Titania mol * % of dopant)	Mass (molar mass of dopant * no. of dopant moles)
SnCl ₂ .2H ₂ O	0.25	1.25*10 ⁻⁵ moles	0.002g
	0.50	2.50*10 ⁻⁵ moles	0.005g
	0.75	3.75*10 ⁻⁵ moles	0.008g
In(NO ₃) ₃ .xH ₂ O	0.25	1.25*10 ⁻⁵ moles	0.003g
	0.50	2.50*10 ⁻⁵ moles	0.007g
	0.75	3.75*10 ⁻⁵ moles	0.011g

- Molar mass of SnCl₂.2H₂O = 225.63g/mol
- Molar mass of In(NO₃)₃. xH₂O = 300.83g/mol

2.3.3 Synthesis of Titania Nanoparticles

Method

2.3.3.1 Sol-gel synthesis

Following sol-gel route and refluxing was adopted from previous work done by Dr. Sofia Javed [101]. The novelty was the introduction of metal dopants Sn and In to know their effects on photocatalytic activities of titania. 2.4g of glacial acetic acid (Sigma-Aldrich) was added as modifier to 11.4g of the precursor, titanium (IV) tetraisopropoxide (TTIP) (97% Aldrich) and put to stirring at room temperature for 10 minutes (Fig.2.11). Then 58ml of distilled water was added quickly with vigorous stirring which resulted in instant formation of precipitation of white color (Fig.2.12). It was left for 1 hour of stirring at room temperature to ensure complete hydrolysis. After that, 0.8ml of concentrated nitric acid (HNO₃) was added to the mixture and it was

heated to 80°C from RT within about 30 minutes time and then peptized for 75 minutes. Total volume was kept 75ml by adding distilled water [101].

2.3.3.2 Refluxing

After that the sol was refluxed for 24 hours at 100°C, after adding different weight percentages of Sn and In doping as given in Table 2.2 (Fig. 2.13.)

2.3.3.3 Drying

The resulted sol was then subjected to drying at 80°C in order to remove water. The dried titania powder resulted.

Table.2.3. Various sol-gel samples with varying type and amount of doping

Sr. No.	Samples	Doping
1	TiO ₂	Un-doped titania
2	A1	0.25 wt% Sn
3	A2	0.50 wt% Sn
4	A3	0.75 wt% Sn
5	B1	0.25 wt% In
6	B2	0.50 wt% In
7	B3	0.75 wt% In

2.3.3.4 Pestle and Mortar

After drying, dried powder samples were properly grinded with pestle and mortar to ensure fine powder of doped and un-doped titania samples (Fig.2.14.)

2.3.3.5 Annealing

Annealing of the dried and grounded samples were done at 450°C for 40 minutes in Nabertherm GmbH N17/ HR – 400V Muffle furnace at heating rate of 1.8 °C/minute (Fig. 2.10)

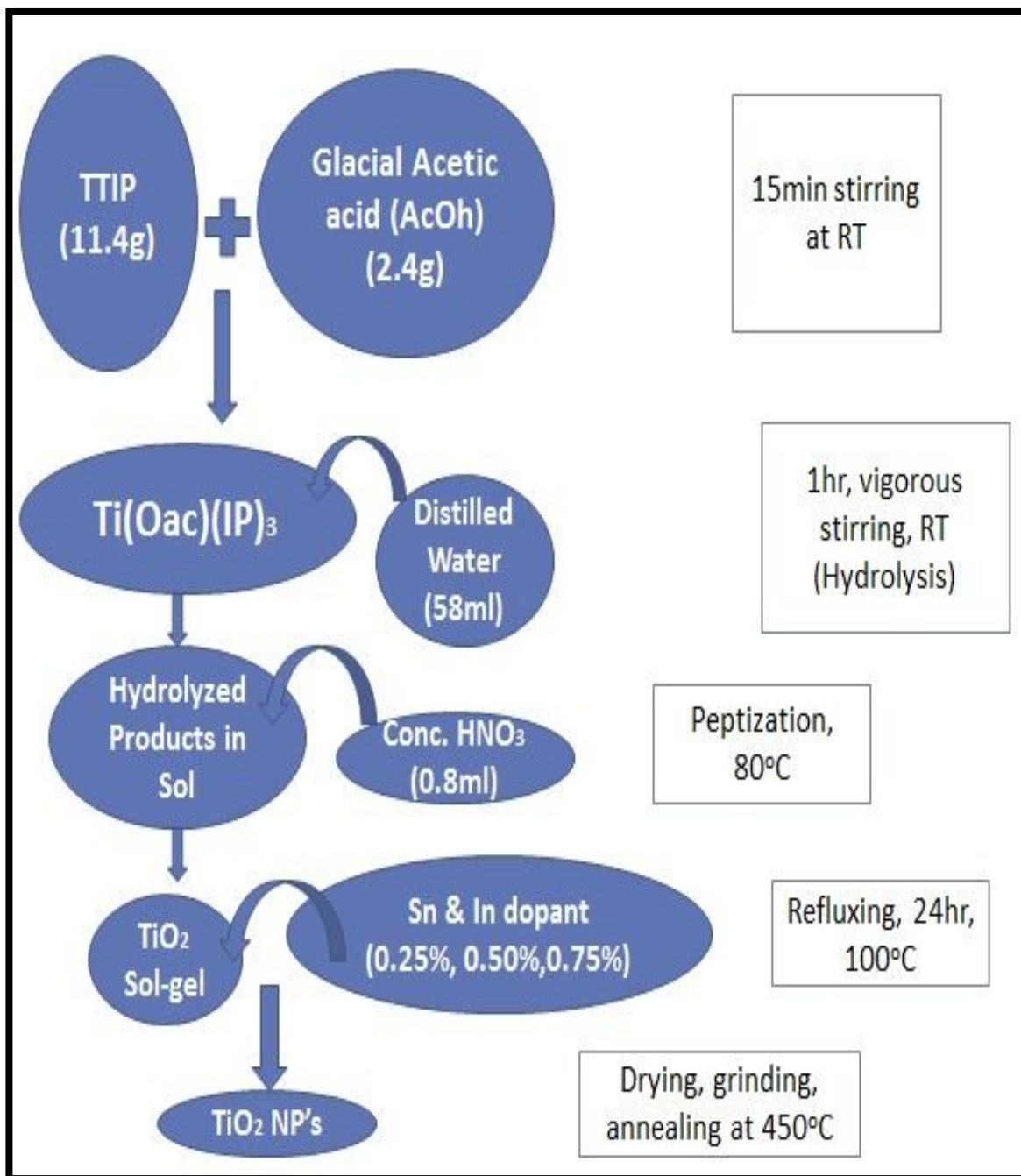


Fig.2.1. Flow sheet for titania nanoparticles synthesis



Fig. 2.2. Mixing of precursor and chelating agent



Fig.2.3. Formation of white precipitation upon adding water (hydrolysis)



Fig.2.4. Sol-gel after refluxing



Fig.2.5. Titania nano powder formed after drying, grinding and annealing

Chapter-3

Characterization

3.1 XRD Analysis

X-ray diffraction (XRD) technique was primarily used to identify and characterize material depending on their diffraction pattern. XRD is based on dual nature of x-ray wave to extract structural information of crystalline materials.

In our work, gel was dried at 80°C and grinded to make fine powder which was exposed to X-rays in Stoe D-64295 Darmstadt X ray Diffractometer for inspecting the material (Fig.3.1), its phase and average crystallite size. The powder was annealed at 450°C for 40 minutes and analyzed for phase and crystallite size.



Fig.3.1. XRD available in SCME,NUST

3.2 Scanning Electron Microscopy

SEM technique is utilized to know the surface morphology and microstructure of the specimen at a higher resolution. Firstly, a specimen is made conductive by employing conducting layers like gold, platinum or carbon etc. to avoid charging during examination from their surface.

An electron beam is targeted onto the specimen. Formation of X-rays backscattered and secondary electrons result due to attack of electron beam on the sample.

In our work, powder sample was diluted with distilled water and put to sonication for an hour and half. Samples were then gold sputtered using copper stub. And then it was observed in JEOL JSM 6490A SEM. Dispersion in dispersants like distil water were made for observing the morphology of the particles. (Fig.3.2)



Fig.3.2. SEM instrumentation

3.3 Fourier Transform Infrared Spectroscopy

Fourier transform infra-red spectrometer (FTIR) is employed for revealing functional groups in organic and inorganic compounds. Technique is not very complex. A monochromatic beam of infrared-radiation when incident on the specimen is transmitted and then collected by the detector. The spectrum as extracted from TIR depicts absorption and transmission from molecules. This technique is very fruitful as no two different molecules possess same kind of spectrum.

In our work, powder samples were mixed with IR grade of KBr in 1:100 to form billets in hydraulic press (Fig.3.3).



Fig.3.3 Hydraulic Press for making Billets for FTIR

Then these billets were inspected under Perkin Elmer Spectrum 100 series FTIR instrumentation (Fig 3.4). FTIR analysis was done to find out the functional groups present in the doped and un-doped sol-gel reflux synthesized titania nanocrystallines.



Fig.3.4. FTIR instrumentation

3.4 UV-Vis Spectroscopy

UV-Visible spectroscopy refers to the absorption spectroscopy in UV-Visible range of 200-1100nm spectra. This electromagnetic region of spectrum results in electronic transitions of atoms and molecules.

In our case, 2mg powder samples were mixed with 5ml of distilled water and sonication was done for 15 minutes. After that, samples were placed in cuvettes and were observed for UV-Vis absorbance and transmittance in T-60U PG Instruments UK having wavelength range of 190-1100nm (Fig.3.5). UV-Visible spectroscopy was done for quantitative optical analysis of doped and un-doped titania powder samples.



Fig.3.5. UV-Vis instrumentation available in IESE,NUST

3.5 Atomic Force Microscopy

Atomic force microscopy (AFM) is the scanning method employed to find out the particle size or surface roughness of the material.

In our research, powder samples in amount of 2mg were dispersed in 10ml distilled water and were put to sonication for an hour to get complete dispersion. After sonication, drops were dropped on glass slides and dried under lamp. Glass slides were later introduced in JSPM 5200 AFM instrumentation (Fig.3.6). AFM was done not for finding out surface roughness in our case as the samples were in powder form, but for particle size analysis.



Fig.3.6. AFM instrumentation

3.6 BET Surface Area Analyzer

Brunauer–Emmett–Teller (BET) surface analysis theory is used to find out the surface area of the material based on the physical adsorption of the gas molecules on the solid surface.

In this work, around 0.5g of dried and annealed powder samples were degassed for about 3 hours and with temperature of 300°C and p/p⁰ range of 0.05 to 0.3 samples were introduced in ‘micromeritics –Gemini VII 2390t’ for surface area analysis (Fig.3.7).



Fig.3.7. BET surface area analyzer

3.7 Raman Spectroscopy

Molecules are identified in Raman spectroscopy by their characteristic structural fingerprints. Vibrational, rotational and other low-frequencies modes in a system are observed by Raman spectroscopy to find out these structural fingerprints (Fig.3.8)

In our work, dried and annealed samples were placed in Raman spectroscopy available in COMSATS Institute of Information Technology, Islamabad. From structural fingerprints, the characteristic vibrational modes phase of the powder was analyzed.



Fig.3.8. Raman Spectroscopy Instrumentation

3.8 Photocatalytic Degradation

Photocatalytical degradation studies were done on methylene blue dye. Stock solution of methylene blue was prepared by adding 1mg of methylene blue in 100ml of RO water. Samples for photocatalytical degradation studies were done prepared by adding 3mg of doped and un-doped titania nano powder in 5ml of methylene blue (MB) solution. Samples were immediately covered to avoid exposure to light. After 15 min of sonication, samples were placed in UV-lamp chamber (Fig.3.9 & Fig.3.10) having wavelength range of 200nm to 280nm for an hour. After one hour samples were checked for photocatalysis degradation by absorbance in UV-Vis spectrometer at 664nm (Methylene Blue Peak Value). Samples were inspected for 8 hours.



Fig.3.9 Photo Catalysis Chamber Facility in IESE, NUST



Fig.3.10. UV lamp chamber

Chapter-4

Results & Discussion

4.1 Synthesis of Titania Nanoparticles

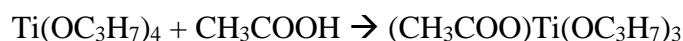
Alkoxide sol-gel was employed to prepare titania nanoparticles utilizing titanium tetraisopropoxide (TTIP) as precursor which is modified with acetic acid. Sol-gel is carried out in solution form offering advantages as low processing temperature and molecular level homogeneity. It is specifically used for synthesis of metal complex oxides like TiO₂ [107]. Reflux condensation was used instead of autoclaving in this research work.

4.1.1 Mechanism of Sol gel Synthesis

Typically in sol gel method, hydrolysis of a metal alkoxide is followed by subsequent condensation (gelation) resulting in the bridging of metal and oxygen O-Ti-O i.e the production of oxide product [107]. Since hydrolysis rates of TTIP are quite high so it was modified using acetic acid before hydrolysis and condensation.

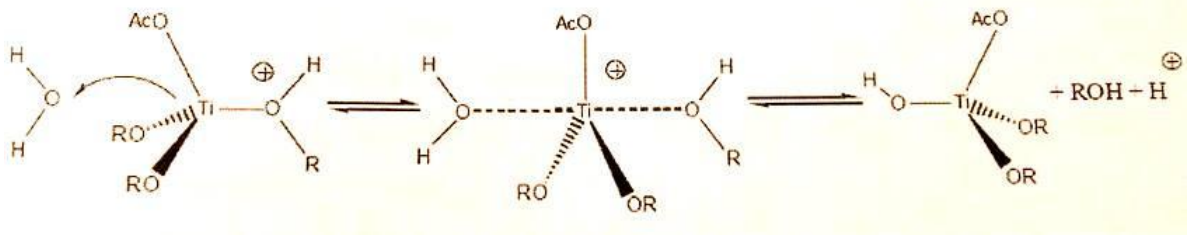
4.1.1.1 Acetic acid modification of TTIP

TTIP and acetic acid were used in the molar ratio of 1:1 and by their ligand exchange we achieve substitution of one of the isopropoxide ligand obtaining titanium acetyl tris iso isopropoxide (TATIP).



The acetic acid not only modifies the precursor but also catalyze the hydrolysis step [111]. Acetate group is less hydrolysable than isopropoxide group giving better control over reaction kinetics. The solution is clear after this step [108-111].

Upon adding water, hydrolysis of TATIP occurs in unimolecular nucleophilic substitution reaction. Ti metal are attacked by oxygen carrying water molecules creating a transition state resulting in hydrolysed products as shown below.



For TATIP adding water with vigorous stirring the mixture at once became white due to precipitation of hydrolysed product. After addition of conc. Nitric acid and peptization titania sol is obtained which had a blue tinge. Sn and In doping in wt% of 0.25, 0.50 and 0.75 was done after peptization (Table.4.1). The sol was refluxed at about 100°C for 24 hours to grow and stabilize the nanoparticles.

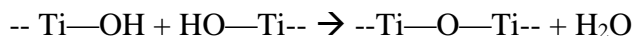


Table.4.1. Description of samples

No.	Alkoxide	Modified Precursor	Refluxing duration (hrs)	Doping	Sample Title
1	TTIP	TATIP	24	Un-doped	TiO ₂
2				0.25% Sn	A1
3				0.50% Sn	A2
4				0.75% Sn	A3
5				0.25% In	B1
6				0.50% In	B2
7				0.75% In	B3

Further insight is obtained via following characterization.

4.2 Scanning Electron Microscopy

Scanning Electron Microscopy (SEM) of the doped and un-doped titania samples were done by JEOL JSM-6490A SEM in SCME NUST. Powder samples weighing 2mg were put into vials containing 10ml of distilled water. The vials were subjected to sonication for about an hour. After preparing SEM samples the following images were obtained. (Fig 4.1 to Fig 4.7).

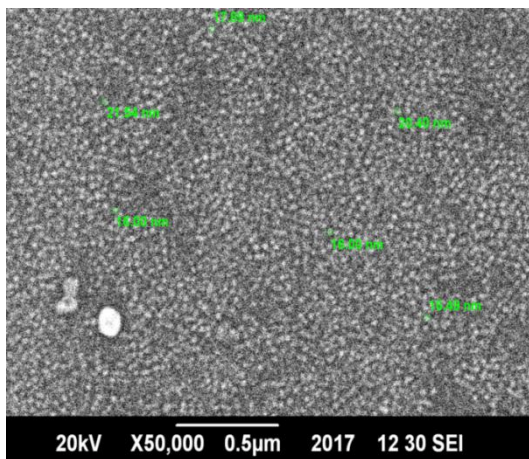


Fig. 4.1. SEM image for Pure TiO_2 Sample

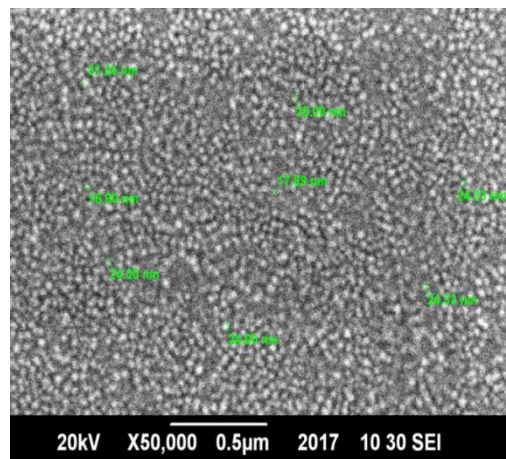


Fig. 4.2. SEM image for 0.25% Sn doped TiO_2 Sample

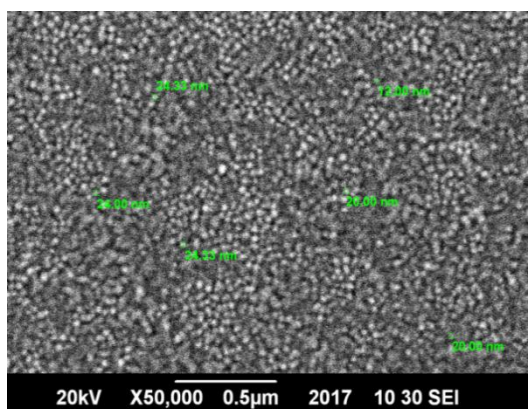


Fig. 4.3. SEM image for 0.50% Sn doped TiO_2 Sample

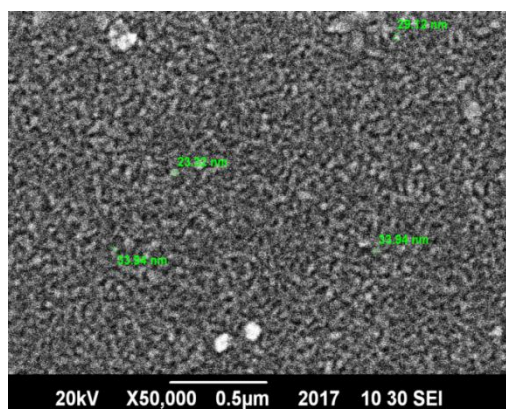


Fig. 4.4. SEM image for 0.75% Sn doped TiO_2 Sample

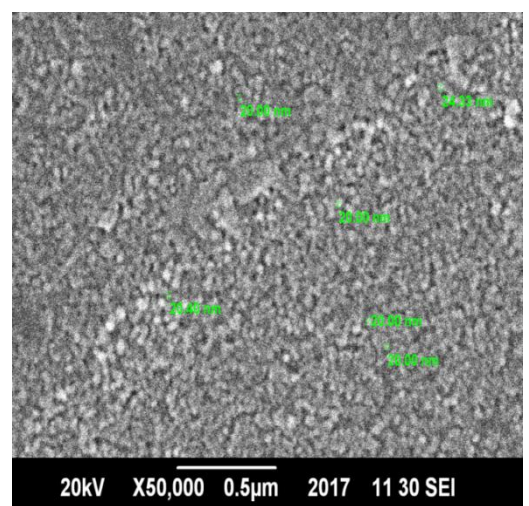


Fig. 4.5. SEM image for 0.25% In doped TiO_2 Sample

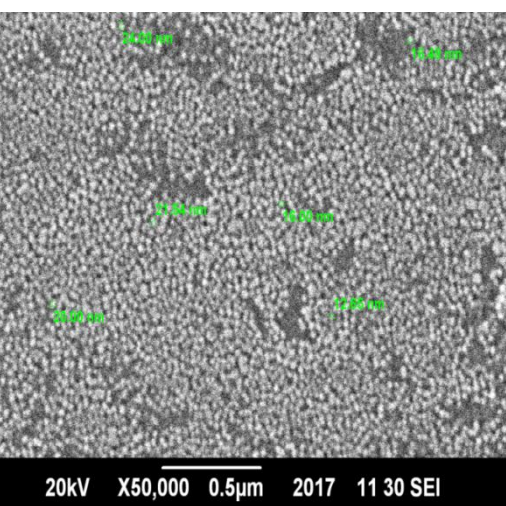


Fig. 4.6. SEM image for 0.50% In doped TiO_2 Sample

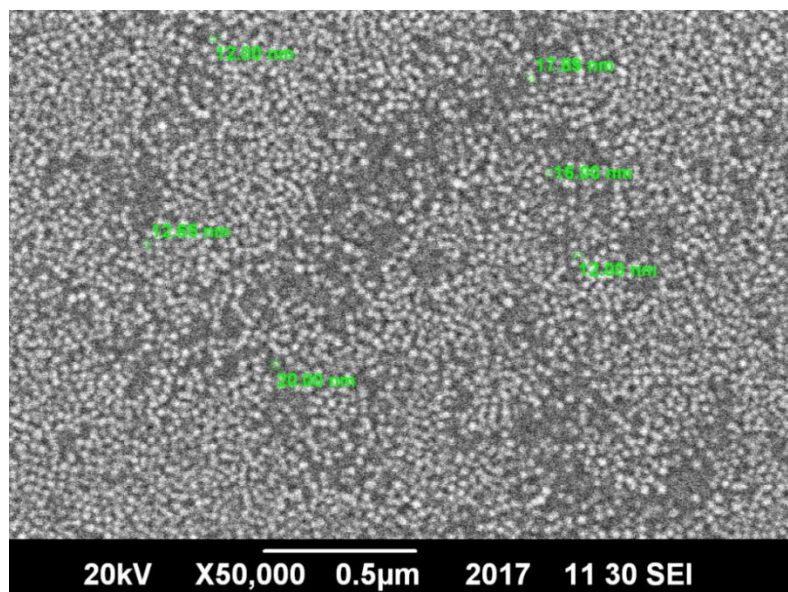


Fig. 4.7. SEM image for 0.75% In doped TiO₂ Sample

As can be seen from above figures, all the samples have particle size of around 20nm approximately. Our SEM images overall shows absolute perfect particle size i.e 12-20nm. Pure titania sample have particle size of 16-20nm (Fig 4.1). Doping with tin and indium haven't changed particle size so much having the particle size range from 12-22nm (Fig 4.2 to Fig 4.7). The mean of particle size ranges revealed in samples is as such depicted in following Table.4.2

Table.4.2. Particle Sizes as revealed by SEM

Sample	Particle size (nm)
Un-doped TiO ₂	22
0.25% Sn	20
0.50% Sn	20
0.75% Sn	19
0.25% In	18
0.50% In	16
0.75% In	12

In both the doped and un-doped sol-gel reflux synthesized titania nanoparticles the morphology revealed by SEM images is of spherical particles having sizes as given in above Table. The reason for forming spherical shaped structure is due to the

restructuring of the material by the thermal energy provided during refluxing. Condensation can also be the reason behind this spherical shaped morphology. Also it is noted that there is a uniformity of morphology throughout the structure of both doped and un-doped samples. The monodispersed particles indicate that they are stabilized and their spherical morphology indicates minimum surface area and thus minimum surface energy. Refluxing has probably resulted in complete condensation of the acetates and hydroxyl groups from the hydrolysed product and spherical titania particles are obtained.

By comparison, it can be concluded that un-doped titania nanoparticles haven't changed much in particle size. The only thing that may have changed is particle size range.

As we know particle size smaller than several tens of nanometers are useable for developing new materials as they have good properties like low melting points, high catalytic activity as compared to bulk material counterparts and special optical properties. Therefore, as in our case nanoparticles in the range of 12-22nm were quite desired and are thus useful.

4.3 BET surface area analysis

BET surface area analysis was done using 'micromeritics – Gemini VII 2390t' in SCME, NUST. The purpose was to analyze the surface areas of doped and un-doped prepared samples. The samples were in powder form. The mass obtained for analysis was between 0.2g – 0.8g. After putting the samples in the cuvettes degassing was done for the time period of 3 hours and temperature was 300°C. P/P_o range was given between 0.05 – 0.3. The surface area values for the doped and un-doped annealed titania nanopowders are listed in Table.4.3. The SEM results can be used to analyze these values.

Table.4.3. BET Surface Area Values for Titania Doped and Un-doped Sol-Gel

Sample Code.	Sample Name	Sample mass (g)	BET Surface Area (m ² /g)
TiO ₂	TiO ₂	0.2300	100.4830
A-1	0.25% Sn doped	0.4800	101.1358
A-2	0.50% Sn doped	0.4300	105.9401
A-3	0.75% Sn doped	0.4700	116.9930

B-1	0.25% In doped	0.5321	102.9982
B-2	0.50% In doped	0.8823	104.5035
B-3	0.75% In doped	0.7165	109.8041

The maximum surface area value is for the samples having smallest particle range as revealed by SEM images. The surface area value for un-doped titania is $100 \text{ m}^2/\text{g}$ corresponding to particle size of 22nm. Sample A1 the 0.25wt% Sn doped titania has increment in surface area value as their size is reduced to 20nm as by SEM images. Similar increasing surface area trend with decreasing particle sizes is observed for A2,A3 and for In doped titania nanopowders.

With increased surface area there will be more available surface for secondary catalytic reactions or interaction between pollutants and photocatalyst and thus low electron-hole recombination which ultimately is useful for higher photocatalytic activity.

4.4 Atomic Force Microscopy

Atomic force microscopy (AFM) was done in SCME, NUST. AFM was done to find out the roughness of nanoparticles and particle size. (Fig 4.8 to Fig 4.14) (Table 4.4). The particle sizes as revealed by AFM were found in agreement with results obtained by SEM and BET surface area analysis for both doped and un-doped titania powders. The dispersions of titania powders were made in distilled water. Sonication was done for about an hour, dropped on glass slides and dried before inspecting under AFM.

Image(512) : Topography
7.00 x 7.00 μm x 20.7 nm

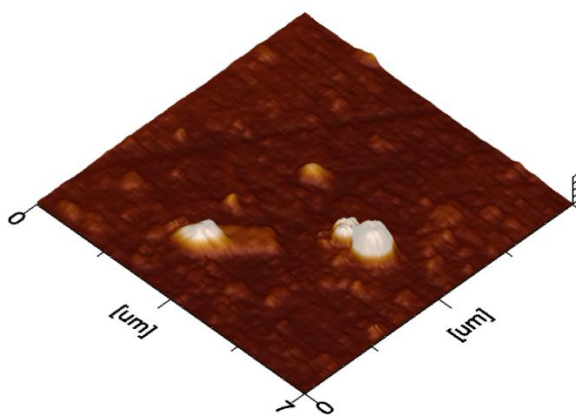


Fig. 4.8. Topography for sol-gel reflux synthesized pure titania

Image(512) : Topography
7.00 x 7.00 μm x 223.0 nm

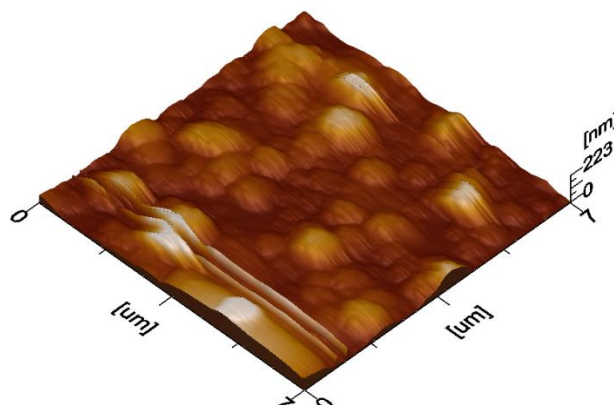


Fig. 4.9. Topography for 0.25% Sn doped sol-gel reflux synthesized titania

Image(512) : Topography
7.00 x 7.00 μm x 97.1 nm

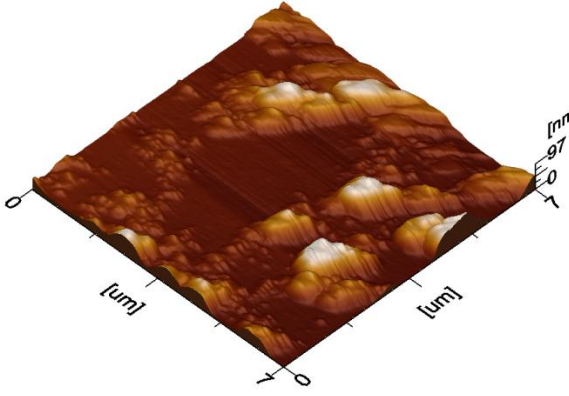


Fig. 4.10. Topography for 0.50% Sn doped sol-gel reflux synthesized titania

Image(512) : Topography
7.00 x 7.00 μm x 164.5 nm

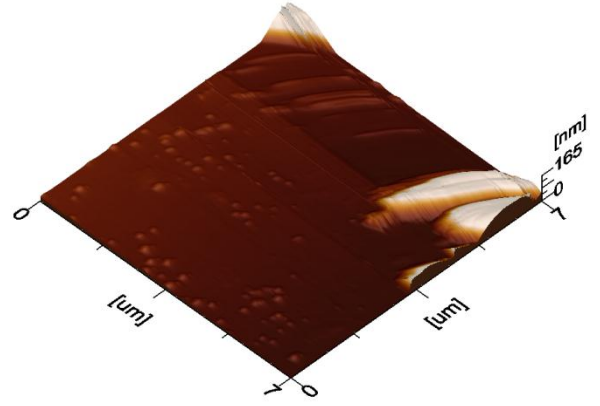


Fig. 4.11. Topography for 0.75% Sn doped sol-gel reflux synthesized titania

Image(512) : Topography
7.00 x 7.00 μm x 71.0 nm

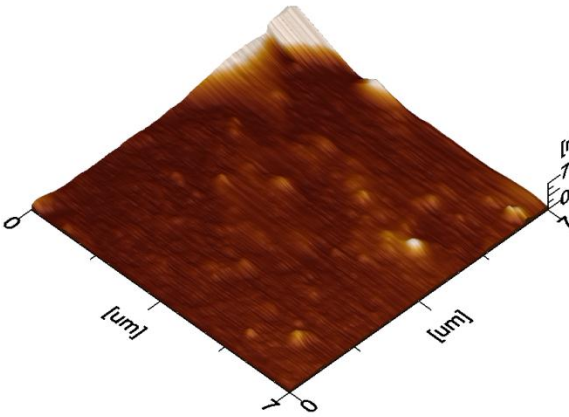


Fig. 4.12. Topography for 0.25% In doped sol-gel reflux synthesized titania

Image(512) : Topography
9.00 x 9.00 μm x 245.9 nm

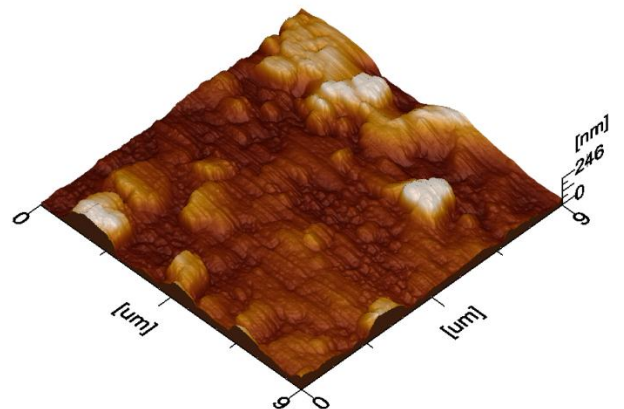


Fig. 4.13. Topography for 0.50% In doped sol-gel reflux synthesized titania

Image(512) : Topography
9.00 x 9.00 μm x 165.2 nm

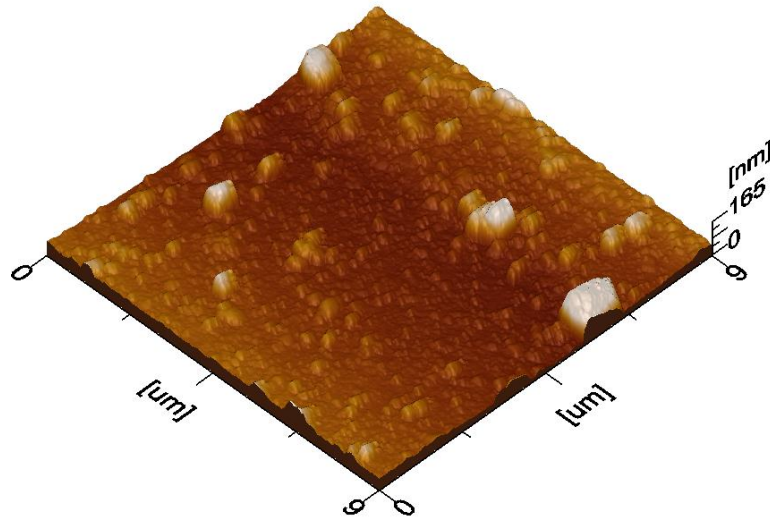


Fig. 4.14. Topography for 0.75% In doped sol-gel reflux synthesized titania

Table 4.4. Particle size for doped and un-doped sol-gel reflux synthesized titania

Sample Code.	Sample Name	Z ₁ -Z ₂ (nm)
TiO ₂	TiO ₂	21
A-1	0.25% Sn doped	21
A-2	0.50% Sn doped	21
A-3	0.75% Sn doped	20
B-1	0.25% In doped	19
B-2	0.50% In doped	17
B-3	0.75% In doped	17

As can be seen in above AFM images and table that particle size is reduced with increasing dopant percentage, which are exactly the results obtained by SEM and BET surface area analysis. Usually AFM is done for surface roughness measurements. But, as in our case samples were dried titania powders we used AFM as an additional option for particle size measurements. Decreasing particle sizes with increasing doping percentage is good indication for better photocatalytic activities as surface area will be increased.

4.5 X-Ray Diffraction

X-ray diffraction (XRD) analysis of the doped and un-doped sol-gel reflux synthesized titania was done in SCME, NUST. XRD was done to find out the phase of prepared titania sol-gels and crystallite sizes. (Fig. 4.15) (Table.4.5.)

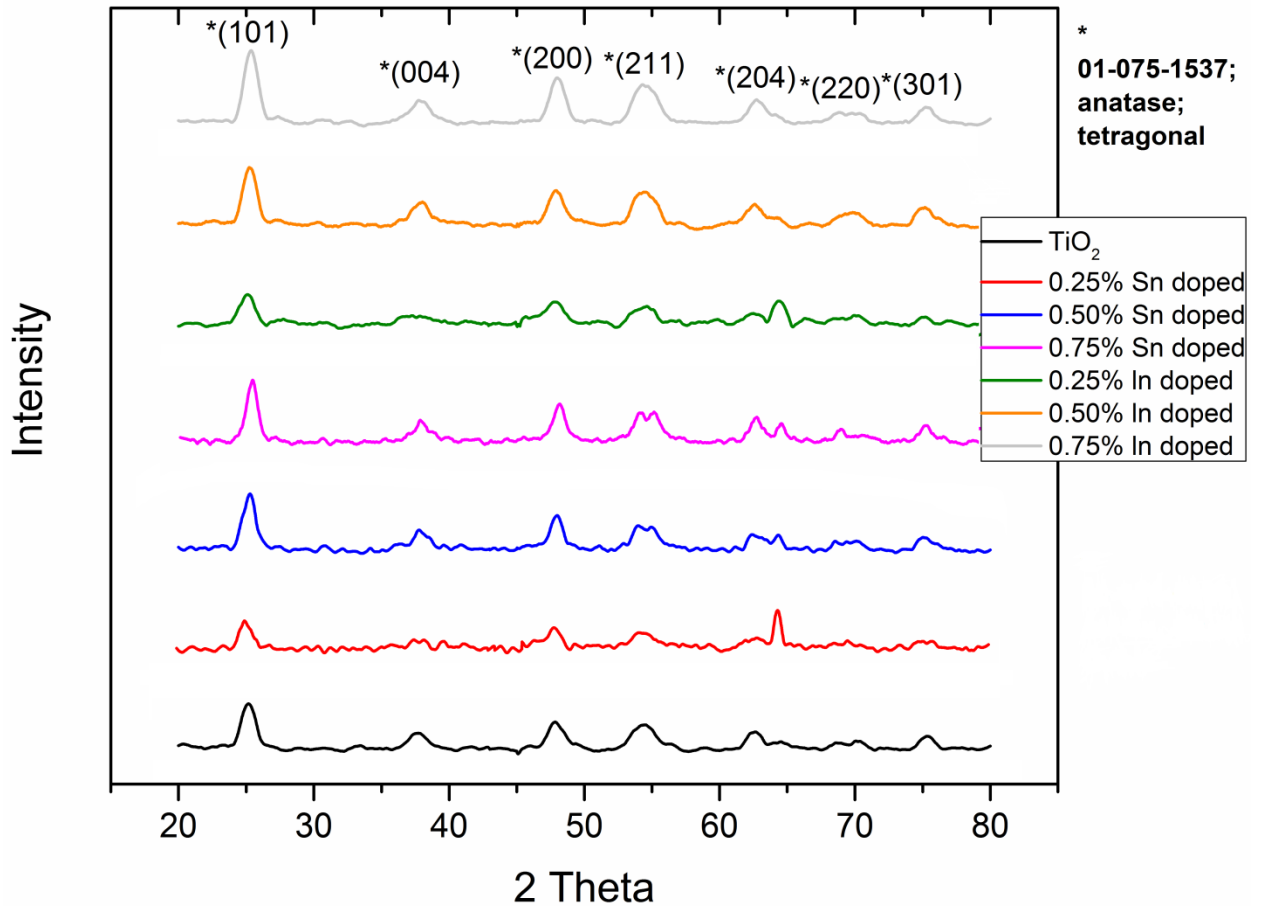


Fig. 4.15. XRD plot for doped and un-doped sol-gel reflux synthesized titania

The XRD results indicate that the material is titania with all the peaks matching with those of anatase phase. All the Sn and In doped and un-doped titania samples show the peaks at 2θ of 25.28° , 38.08° , 47.92° , 53.32° and 62.66° which are assigned to (101), (004), (200), (211) and (204) lattice planes of anatase phase titania.

The increase in peak intensity indicates the presence of crystalline structures. As samples were annealed there were no peaks other than for that of anatase phase. Heat treatment i.e annealing has burnt out all the organic content as it is the inherent nature of

sol-gel method. The major peaks found are in accordance to anatase phase of titania as found by X'Pert High Score Software (i.e # 01-075-1537).

Scherer equation: $t = 0.94 \lambda / B \cos \theta$; where, t = crystallite size, B = peak width at half maximum, θ = diffraction angle, was used to crystallite size. It was found to be less than 20nm approximately for all doped and un-doped titania values. (Table 4.5)

Table 4.5. Crystallite size of doped and un-doped sol-gel reflux synthesized titania

Sample Code.	Sample Name	Crystallite Size (nm)
TiO ₂	TiO ₂	19.5
A-1	0.25% Sn doped	18.1
A-2	0.50% Sn doped	16.1
A-3	0.75% Sn doped	14.1
B-1	0.25% In doped	12.6
B-2	0.50% In doped	11.5
B-3	0.75% In doped	10.9

Thus the values of crystallite size as found by XRD show nano crystallinity. Crystallite sizes as obtained here are in agreement to the surface area values using BET analyzer and particle sizes as revealed by SEM and AFM.

4.6 Raman Spectroscopy

Raman spectroscopy was done at COMSATS Institute of Information Technology (CIIT), Islamabad. The phase of titania was analyzed by Raman Spectroscopy. From the results obtained characteristics peaks E_{1g} , B_{1g} (non-symmetric vibration mode), A_{1g} (symmetric vibration mode) and E_{3g} at 115,371,494 and 619 cm^{-1} are peaks for anatase phase of titania. There are however change in the intensity of the peaks which is

attributed to the change in effect extracted by samples of heat treatment, roughness of starting material, particle size variations and distributions. (Fig. 4.16).

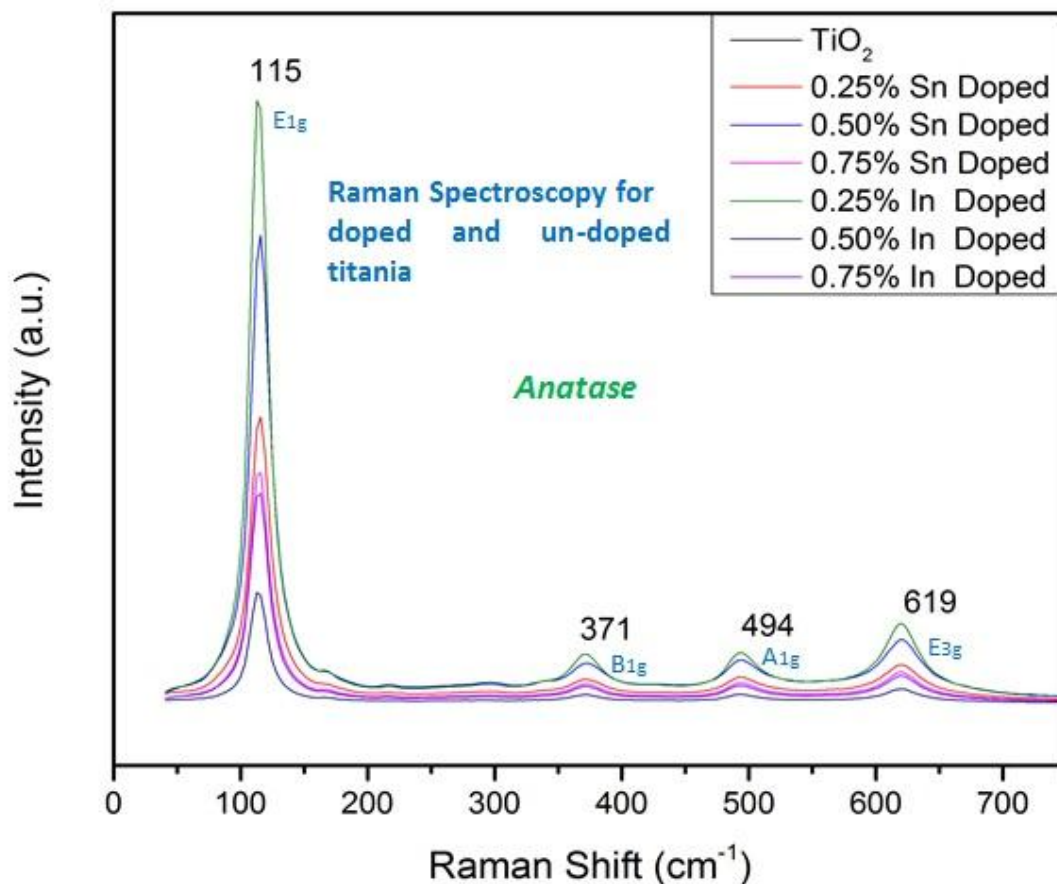


Fig 4.16. Raman shifts for doped and un-doped sol-gel reflux synthesized titania

The phase as revealed by the Raman spectroscopy is in accordance with the phase identified from the XRD results of both doped and un-doped titania nanopowders.

4.7 UV-Vis Spectroscopy

UV- Vis spectroscopy of the doped and un-doped samples were done in IESE,NUST. Following absorption and transmittance spectrums were obtained (Fig. 4.17 and Fig. 4.18).

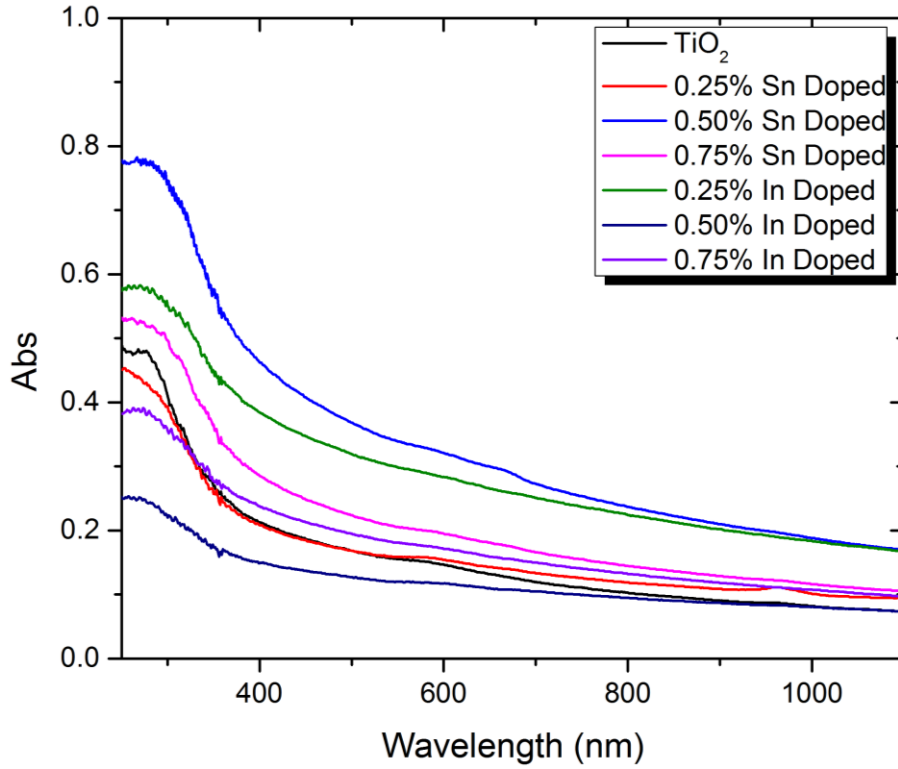


Fig. 4.17. UV-Vis absorption spectrum for doped and un-doped sol-gel reflux synthesized titania

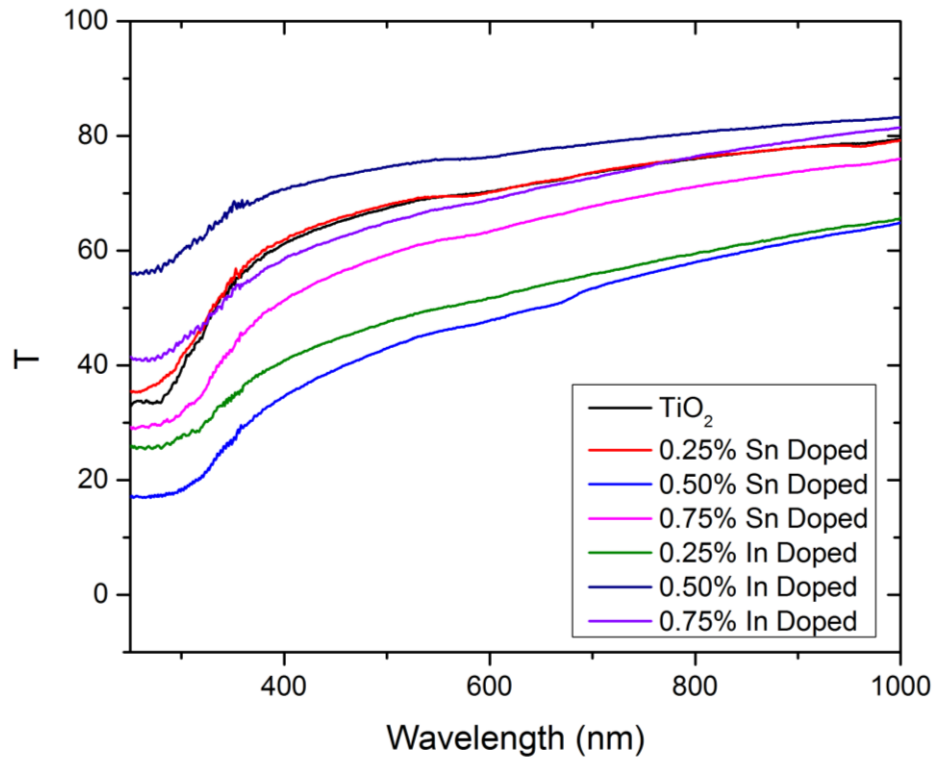


Fig. 4.18. UV-Vis Transmittance spectrum for doped and un-doped sol-gel reflux synthesized titania

UV-visible absorption and transmittance spectrum for Sn doped and un-doped titania (Fig.4.17 and Fig.4.18.) reveal that pure TiO₂ shows has a strong peak at 350nm, due to the electronic transition from the valence band (VB) to the conduction band (CB) of TiO₂ [112]. The band threshold at 400nm corresponds to the band gap of 3.31eV as can be seen from Tauc's plot for pure titania in Fig.4.19. For 0.25% Sn & In doped TiO₂ sample absorption peak at 350nm correspond to the band gap of 3.19 & 3.07 eV respectively (Fig.4.20 & Fig.4.23.). This peak is attributed to the band-band transition of TiO₂, which have slight shift compared with pure titania. A broad range absorption from 400nm-800nm is observed in 0.25% Sn & In doped titania samples. Almost same is the case with 0.50% and 0.75% Sn & In doped titania samples having absorptions peaks at 350nm and band gaps of 3.11eV,3.04eV and 3.09eV,2.97eV respectively (Fig.4.21, 2.22 & Fig.4.24 ,4.25). Visible region absorption increases with the increment in Sn & In ions doped in TiO₂. It is therefore stated that extraordinary absorption at 400nm-800nm is related to the Sn & In doping into titania. Note that there is approximately 10% loss in transmittance at all wavelengths, which is attributed to all materials transmittance done under UV-visible spectroscopy (Fig.4.18).

The band gap energy values as determined from Tauc plots (Fig.4.19-4.25) are listed in Table.4.6. Decrease in the band gap values with increasing dopant amount indicates that less energy will be required by photons to create photo-excited electron-hole pair for photocatalytic activity.

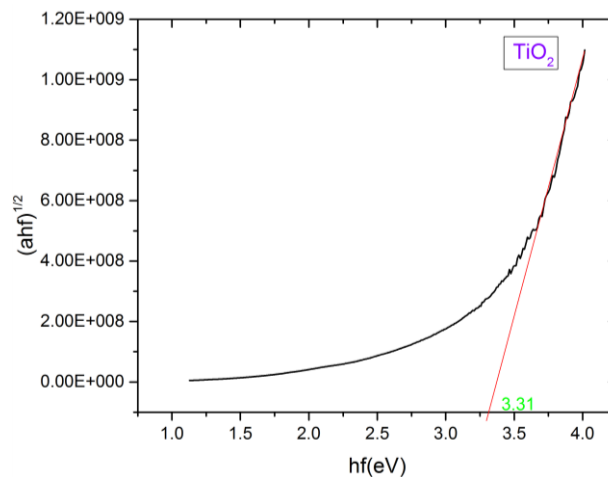


Fig. 4.19. Tauc's plot for sol-gel reflux synthesized pure titania

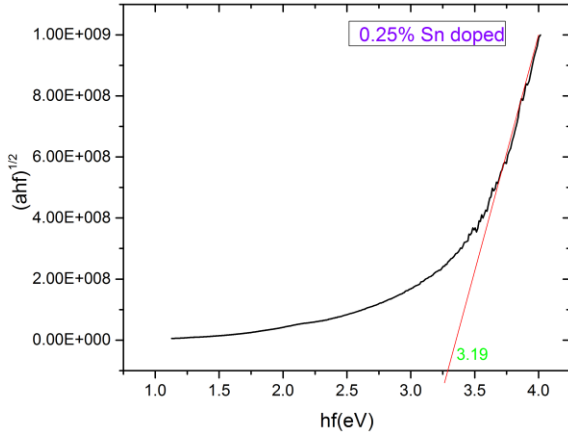


Fig. 4.20. Tauc's plot for 0.25% Sn doped sol-gel reflux synthesized doped titania

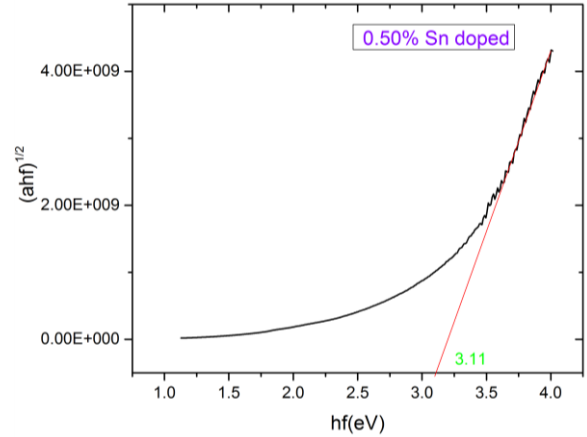


Fig. 4.21. Tauc's plot for 0.50% Sn doped sol-gel reflux synthesized doped titania

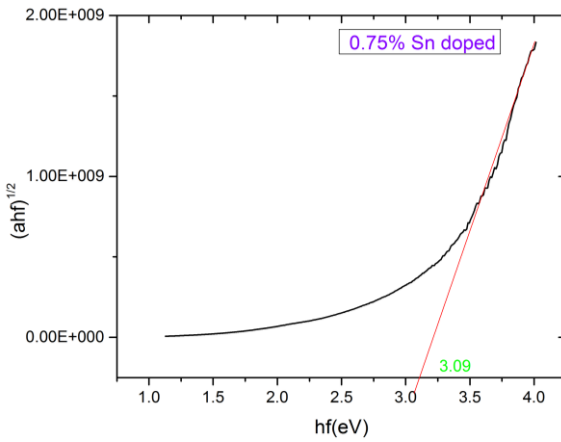


Fig. 4.22. Tauc's plot for 0.75% Sn doped sol-gel reflux synthesized doped titania

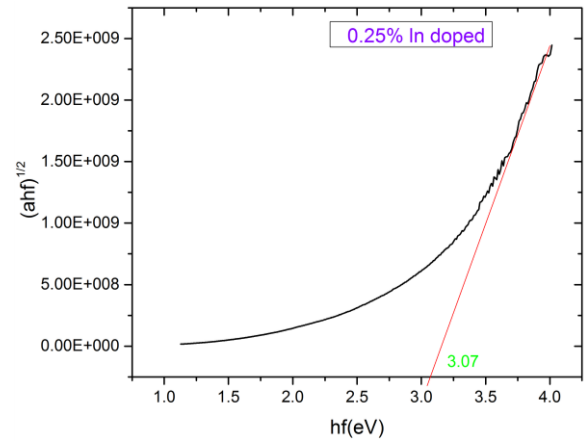


Fig. 4.23. Tauc's plot for 0.25% In doped sol-gel reflux synthesized doped titania

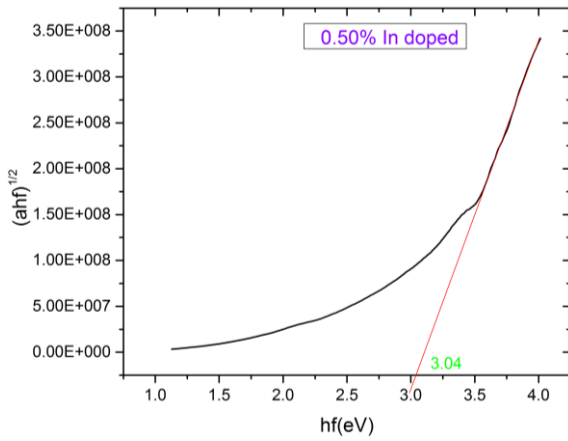


Fig. 4.24. Tauc's plot for 0.50% In doped sol-gel reflux synthesized doped titania

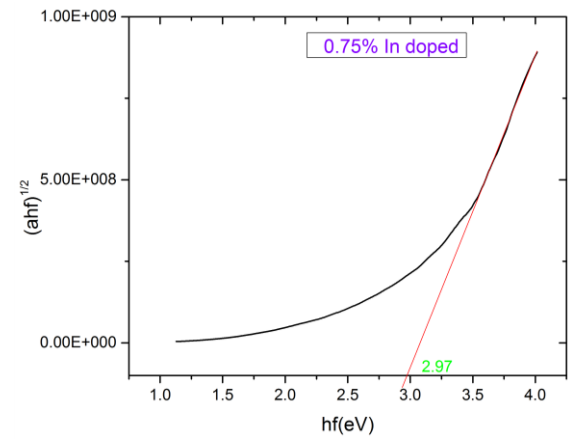


Fig. 4.25. Tauc's plot for 0.75% In doped sol-gel reflux synthesized doped titania

Table.4.6. Band gap values by Tauc's plot for doped and un-doped titania samples

Sample	Bandgap (eV)
Un-doped TiO ₂	3.31
0.25% Sn	3.19
0.50% Sn	3.11
0.75% Sn	3.09
0.25% In	3.07
0.50% In	3.04
0.75% In	2.97
Mean \pm SD	3.11 \pm 0.11

4.8 Fourier Transform Infrared Spectroscopy

Fourier transform infrared spectroscopy (FTIR) of doped and un-doped sol-gel reflux synthesized samples was done in SCME, NUST. FTIR was done to find out the functional group and bonding in the samples (Fig. 4.26). (Table. 4.7) showing the frequency ranges of the functional groups present

As revealed by the FTIR results, we have C-H stretching peak at 2900cm⁻¹ which is due to the precursor or alkoxide i.e TTIP. The peak at 163cm⁻¹ is for carbonyl group (COO) which is due to the modifier i.e acetic acid. Anatase phase was revealed due to its frequency values at 669cm⁻¹ showing Ti-O vibrations. Peak at 3437cm⁻¹ is of hydroxyl group due to the molecular water and O-H group present. Ti-O-Ti peak was indicated having peak at 1400cm⁻¹. Thus, the results as revealed by FTIR shows the formation of bonding Ti-O-Ti i.e TiO₂ and also the phase anatase due to Ti-O bond vibrations.

Table 4.7. Wavenumbers of FTIR peaks in doped and un-doped sol-gel reflux synthesized titania

Functional Group	Wavenumber (cm ⁻¹)
C-H stretch	2900
Ti-O-Ti	1400
COO	1630
Anatase phase	669
Hydroxyl Group	3437

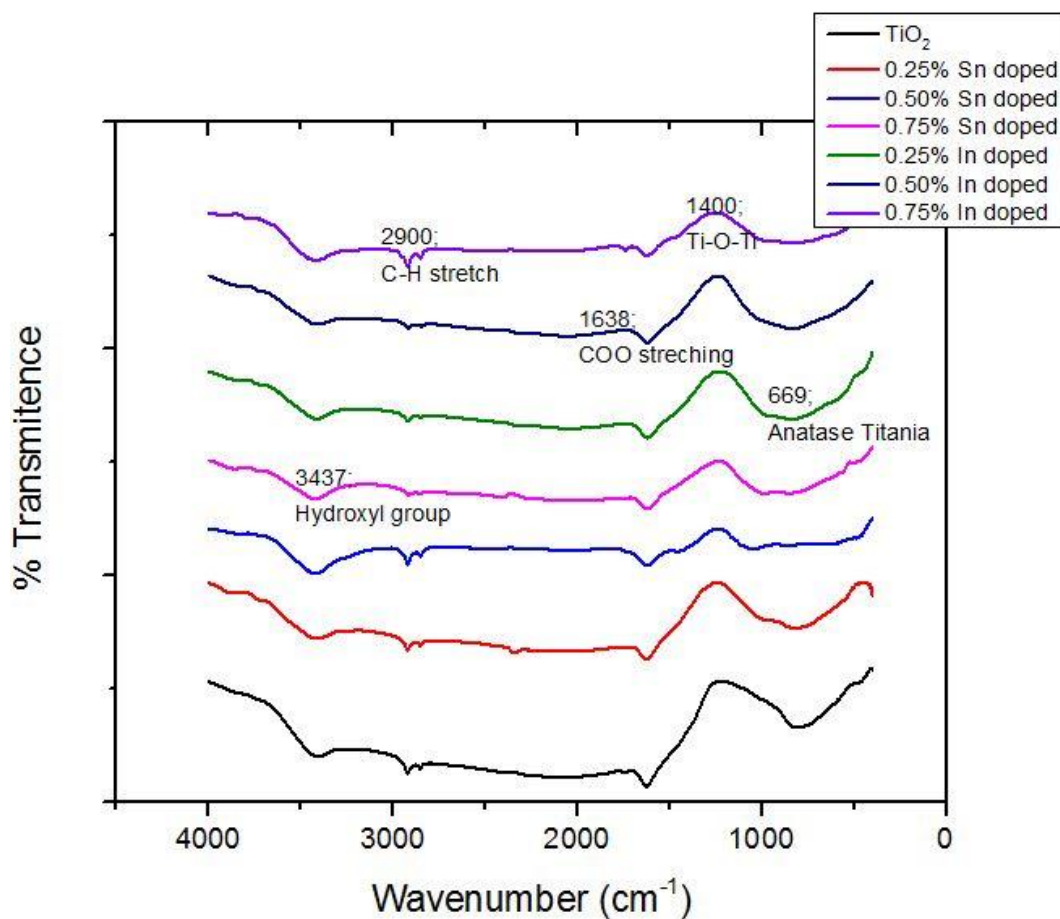


Fig. 4.26. FTIR plot for doped and un-doped sol-gel reflux synthesized titania

4.9 Photocatalytic Degradation

Doped and un-doped titania samples were used to evaluate photocatalytic degradation of methylene blue under UV-lamp. Stock solution of methylene blue was prepared by adding 1mg of methylene blue in 100ml of RO water. Samples for photocatalytic degradation studies were done prepared by adding 3mg of doped and un-doped titania nano powder in 5ml of methylene blue (MB) solution. Samples were immediately covered to avoid exposure to light. After 15 min of sonication, samples were placed in UV-lamp chamber having wavelength range of 200nm to 280nm for an hour. After one hour samples were checked for photocatalytic degradation by absorbance in UV-Vis spectrometer at 664nm (λ_{max}). Samples were inspected for 8 hours.

Following results and trends were observed in Sn (Fig.4.27.) and In (Fig.4.28.) doped samples for photocatalytic degradation of methylene blue.

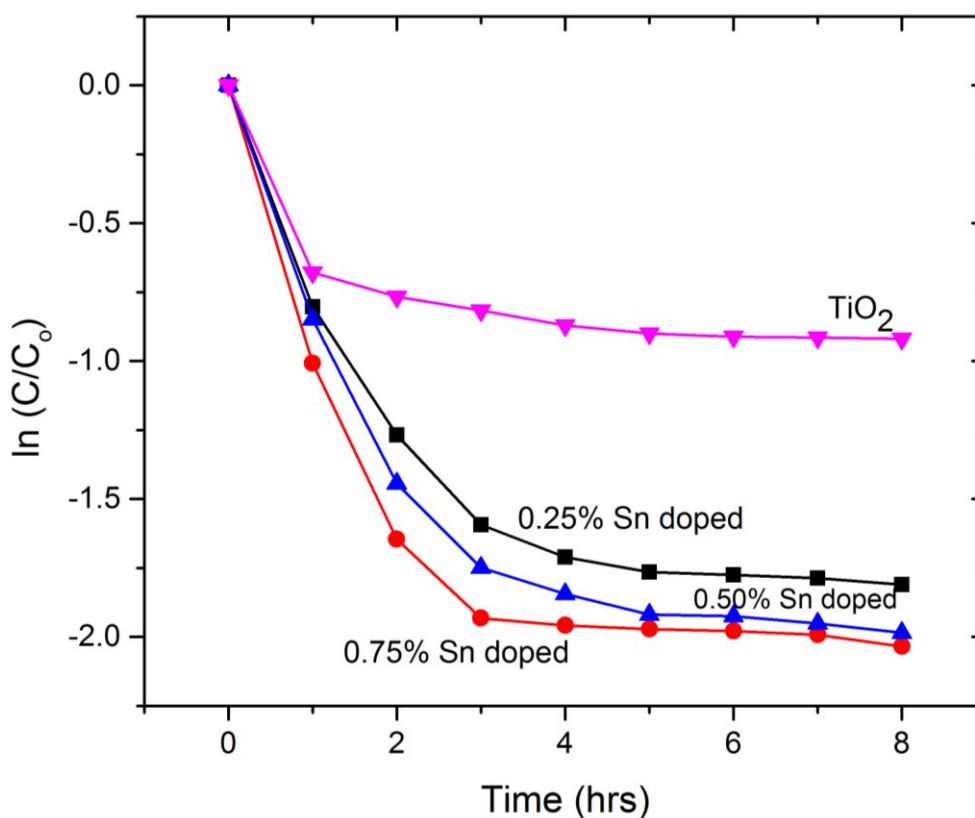


Fig. 4.27 Photocatalysis Degradation of Methylene Blue by Tin doped titania

As can be seen from the above graph, that Sn doped titania samples have reduced the methylene blue concentration with increasing weight percentage of Sn doping

(Fig.4.29), indicating the increase in photocatalytic degradation of dye. There is a proper trend in Sn doped titania samples. 0.25% Sn doped have relatively less photocatalytic activity than 0.50% and similarly 0.5% less than 0.75%. Thus this can be concluded that with increasing Sn doping there is continuous increase in photocatalytic degradation of methylene blue.

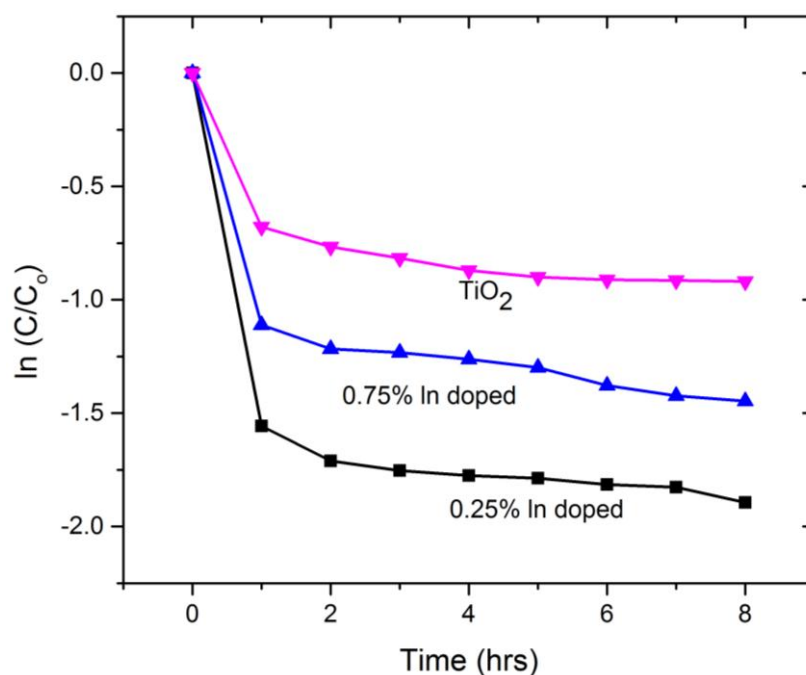


Fig. 4.28. Photocatalytic Degradation of Methylene Blue by Indium doped titania



Fig.4.29. Change in Color & Concentration of MB with time

When talking about photocatalytic activities of In doped titania powders, there is also increasing trend of photocatalytic degradation but 0.25% has better photocatalytic activity than 0.75%.. As can be seen (Fig.4.29.) increasing trend of photocatalytic degradation can be deduced in relation to increased percentage of In doping. 0.75% In doped titania samples have less photocatalytic degradation for methylene blue than 0.25% In doped sample though.

Concluding, both Sn and In doped samples have better photocatalytic degradation of dye than un-doped titania samples. However, both doping have different kind of trends in photocatalytic activities (PA) with respect to wt%. Sn samples have decreasing dye concentration with increasing doping percentage. While for In doping, 0.25% have better PA than 0.75% In doped sample.

Chapter-5

5.1 Conclusions

- Doped and un-doped titania nanocrystalline powders resulted via sol-gel reflux synthesis.
- SEM results showed the particle size range of 12-22nm for both doped and un-doped titania powders.
- There was an increase of nucleation sites with the introduction of dopants thus particles sizes were in nano range
- BET surface area analysis thus showed the increase in surface area for doped samples as compared to un-doped titania sample.
- AFM revealed the same particle sizes as in agreement to the results obtained from SEM and BET surface area analysis.
- Nano crystalline powder was revealed as by XRD.
- Anatase phase was confirmed by XRD and Raman Spectroscopy with no other phase present.
- Functional group analysis as done by FTIR showed the formation of Ti-O-Ti bond.
- There was an increase of absorbance wavelength range with increasing doping for titania as shown by UV-Vis spectra.
- Photocatalytic degradation studies for both Sn and In doped samples were done and results were compared to un-doped titania sample. Following trends were observed;
 - Sn doped titania samples showed good results as with the increase in time and weight percentage doping of Sn, concentration of methylene blue was decreasing i.e enhanced photocatalytic degradation.
 - Similarly, In doped samples showed decrease in concentration of dye however, 0.25wt% has better photocatalytic activity than 0.75wt%.
- Finally we can conclude by stating that, both Sn and In doped (0.25%,0.50%,0.75%) sol-gel reflux synthesized nanocrystalline anatase

samples have enhanced photocatalytic degradation of organic pollutants as it has diluted the concentration of model pollutant i.e methylene blue the dye.

5.2 Future Recommendation

- Sn and In doped sol-gel reflux synthesized titania nanocrystalline powders have the potential to be used for other applications as self-cleaning, solar cells and super capacitors.
- Photocatalytic activity of Sn & In doped titania nano particles can be explored for further studies by varying parameters for example doping %, increasing time for photocatalytic degradation.
- We can use more safer light energy or gas discharge source as Ultraviolet-Light Emitting Diodes (UV-LED's) than hazardous UV-lamps.
- Though some work has been done before on In doped titania , but as Sn doped titania is still almost novel so much can be explored with varying doping weight percentage to find more better and optimum results.
- Studies can be done by varying other parameters like refluxing time, different modifiers e.g acetylene acetone etc

References

- [1] P.R. Gogate, A.B. Pandit, *Adv. Environ. Res.* 8 (2004) 501.
- [2] US EPA, National Emission Standards for Hazardous Air Pollutants, 40 CFR, part 63, 2006.
- [3] C. Guillard, J. Disdier, J.-M. Herrmann, C. Lehaut, T. Chopin, S. Malato, J. Blanco, *Catal. Today* 54 (1999) 217.
- [4] W.A. Zeltner, D.T. Tompkin, *Ashrae Transactions*, vol. III, American Society of Heating and Air-Conditioning Engineers Inc., 2005, part 2, p. 532.
- [5] O. Carp, C.L. Huisman, A. Reller, *Prog. Solid State Chem.* 32 (2004) 33.
- [6] A. Fujishima, K. Honda, *Nature (London)* 238 (1972) 37.
- [7] V. Augugliaro, M. Litter, L. Palmisano, J. Soria, *J. Photochem. Photobiol. C* 7 (2006) 127.
- [8] Lee, S. K.; Mills, A. J. *Ind. Eng. Chem.* 2004, 2, 173–187.
- [9] Mills, A.; Lee, S. K.. *J. Photochem. Photobiol., A* 2002, 152, 233–247.
- [10] Ollis, D.; Pelizzetti, E.; Serpone, N. *Environ. Sci. Technol.* 1991, 25, 1522–1529.
- [11] Hoffman, M. R.; Martin, S. T.; Choi, W.; Bahnemann, D. W. *Chem. Rev.* 1995, 95, 69–96.
- [12] Peral, J.; Domenech, X.; Ollis, D. F. *J. Chem. Technol. Biotechnol.* 1997, 70, 117–140.
- [13] Zhao, J.; Yang, X. *Building Environ.* 2003, 38, 645–654.
- [14] Xianzhi, F.; Walter, A. Z.; Andreson, M. A. *Appl. Catal., B* 1995, 6, 209–224.
- [15] Hyeok, C.; Yong, J. K.; Rajender, S. V.; Dionysios, D. D. *Chem. Mater.* 2006, 18, 5377–5384.
- [16] Li, B.; Wang, X.; Yan, M.; Li, L. *Mater. Chem. Phys.* 2002, 78, 184–188.
- [17] Fujishima, A.; Rao, T. N.; Tryk, D. A. *J. Photochem. Photobiol., C* 2000, 1, 1–21.
- [18] Linsebigler, A. L.; Lu, G.; Yates, J. T., Jr. *Chem. Rev.* 1995, 95, 735–758.
- [19] Tada, H.; Yamamoto, M.; Ito, S. *Langmuir* 1999, 15, 3699–3702.
- [20] Wang, J. A.; Limas-Ballesteros, R.; Lopez, T.; Moreno, A.; Gomez, R.; Novaro, O.; Bokhimi, X. *J. Phys. Chem. B* 2001, 105, 9692–9698.
- [21] Yu, J. C.; Yu, J. G.; Zhao, J. C. *Appl. Catal., B* 2002, 36, 31–42.
- [22] A Fujishima, X Zhang, DA Tryk. *Surface Science Reports*, vol. 63, pp. 515-582, 2008.
- [23] AE Jacobsen. *Industrial and Engineering Chemistry*, vol. 41, pp. 523-526, 1949.
- [24] A Fujishima, K Honda. *Nature*, vol. 238, pp. 37, 1972.
- [25] K Nakata, A Fujishima *Journal of Photochemistry and Photobiology C-Photochemistry Reviews*, vol. 13, pp. 169-189, 2012.
- [26] O Carp, CL Huisman, A Reller. *Progress in Solid State Chemistry*, vol. 32, pp. 33-177, 2004.
- [27] K Maeda. *Journal of Photochemistry and Photobiology CPhotochemistry Reviews*, vol. 12, pp. 237-268, 2011.
- [28] SS Tan, L Zou, E Hu. *Catalysis Today*, vol. 115, pp. 269-273, 2006.
- [29] T Inoue, A Fujishima, S Konishi, K Honda. *Nature*, vol. 277, pp. 637-638, 1979.

- [30] JC Crittenden, RPS Suri, DL Perram, DW Hand. *Water Research*, vol. 31, pp. 411-418, 1997.
- [31] UI Gaya, AH Abdullah. *Journal of Photochemistry and Photobiology C-Photochemistry Reviews*, vol. 9, pp. 1-12, 2008.
- [32] J Peral, X Domenech, DF Ollis. *Journal of Chemical Technology and Biotechnology*, vol. 70, pp. 117-140, 1997.
- [33] S Nishimoto, B Bhushan. *Rsc Advances*, vol. 3, pp. 671-690, 2013.
- [34] F Rupp, M Haupt, H Klostermann, HS Kim, M Eichler, A Peetsch, et al. *Acta Biomaterialia*, vol. 6, pp. 4566-4577, 2010.
- [35] J.-M. Herrmann, *Catal. Today* 53 (1999) 115.
- [36] J. Zhao, X. Yang, *Build. Environ.* 38 (2003) 645.
- [37] N.T. Dung, N.V. Khoa, J.-M. Herrmann, *Inter. J. Photoenergy* 7 (2005) 11.
- [38] K. Vinodgopal, P.V. Kamat, *J. Phys. Chem.* 96 (1992) 5053.
- [39] MA Behnajady, N Modirshahla, M Shokri, B Rad. *Global Nest Journal*, vol. 10, pp. 1-7, 2008.
- [40] OK Dalrymple, E Stefanakos, MA Trotz, DY Goswami. *Applied Catalysis B Environmental*, vol. 98, pp. 27-38, 2010.
- [41] HA Foster, IB Ditta, S Varghese, A Steele. *Applied Microbiology and Biotechnology*, vol. 90, pp. 1847-1868, 2011.
- [42] JW Liou, HH Chang. *Archivum Immunologiae Et Therapiae Experimentalis*, vol. 60, pp. 267-275, 2012.
- [43] I.K. Konstantinou, V.A. Sakkas, T.A. Albanis, *Water Res.* 36 (2002) 2733.
- [44] J. Perkowski, S. Bzdon, A. Bulska, W.K. Jo´ z´wiak, *Polish J. Environ. Stud.* 15(2003) 457.
- [45] A. Fujishima, T.N. Rao, D.A. Tryk, *J. Photochem. Photobiol. C* 1 (2000) 1.
- [46] K. Rajeshwar, C.R. Chenthamarakshan, S. Goeringer, M. Djukic, *Pure Appl. Chem.* 73 (2001) 1849.
- [47] Z. Zhang, P.A. Maggard, *J. Photochem. Photobiol. A* 186 (2007) 8.
- [48] D. Gummy, A.G. Rincon, R. Hajdu, C. Pulgarin, *Solar Energy* 80 (2006) 1376.
- [49] K. Kabra, R. Chaudhary, R.L. Sawhney, *Indian Eng. Chem. Res.* 43 (2004) 7683.
- [50] S. Hunoh, J.S. Kim, J.S. Chung, E.J. Kim, *Chem. Eng. Comm.* 192 (2005) 327.
- [51] S.-Z. Chen, P.-Y. Zhang, W.-P. Zhu, L. Chen, S.-M. Xu, *Appl. Surf. Sci.* 252 (2006) 7532.
- [52] T. Kemmitt, N.I. Al-Salim, M. Waterland, V.J. Kennedy, A. Markwitz, *Curr. Appl. Phys.* 4 (2004) 189.
- [53] L.C. Macedo, D.A.M. Zaia, G.J. Moore, H. de Santana, *J. Photochem. Photobiol. A* 185 (2007) 86.
- [54] H. Kim, S. Lee, Y. Han, J. Park, *J. Mater. Sci.* 40 (2005) 5295.
- [55] Choi, W.; Termin, A.; Hoffmann, M. R. *J. Phys. Chem.* 1994, 98, 13669.
- [56] Ghicov, A.; Macak, J. M.; Tsuchiya, H.; Kunze, J.; Haeublein, V.; Frey, L.; Schmuki, P. *Nano Lett.* 2006, 6, 1080.
- [57] Chen, X.; Mao, S. S. *Chem. ReV.* 2007, 107, 2891.
- [58] Hoffmann, M. R.; Martin, S. T.; Choi, W.; Bahnemann, D. W. *Chem. ReV.* 1995, 95, 69.
- [59] Ding, Z.; Lu, G. Q.; Greenfield, P. F. *J. Phys. Chem. B* 2000, 104, 4815.
- [60] O.K. Dalrymple, D.H. Yeh, M.A. Trotz, *J. Chem. Technol. Biotechnol.* 82 (2007) 121.

- [61] L. Yang, Z. Liu, *Energy Convers. Manage.* 48 (2007) 882.
- [62] Kisch, H.; Zang, L.; Lange, C.; Maier, W. F.; Antonius, C.; Meissner, D. *Angew. Chem., Int. Ed. Engl.* 1998, 37, 3034.
- [63] Zang, L.; Macyk, W.; Lange, C.; Maier, W. F.; Antonius, C.; Meissner, D.; Kish, H. *Chem.sEur. J.* 2000, 6, 379.
- [64] Chang, S.; Doong, R. *J. Phys. Chem. B* 2006, 110, 20808.
- [65] Chen, D.; Jiang, Z.; Geng, J.; Wang, Q.; Yang, D. *Ind. Eng. Chem. Res.* 2007, 46, 2741.
- [66] Cong, Y.; Zhang, J.; Chen, F.; Anpo, M.; He, D. *J. Phys. Chem. C* 2007, 111, 10618.
- [67] Cao, Y.; Yang, W.; Zhang, W.; Liu, G.; Yue, P. *New J. Chem.* 2004, 28, 218.
- [68] Luo, H.; Takata, T.; Lee, Y.; Zhao, J.; Domen, K.; Yan, Y. *Chem. Mater.* 2004, 16, 846.
- [69] Justicia, I.; Ordejon, P.; Canto, G.; Mozos, J. L.; Fraxedas, J.; Battiston, G. A.; Gerbasi, R.; Figueras, A. *AdV. Mater.* 2002, 14, 1399.
- [70] Nakamura, I.; Negishi, N.; Kutsuna, S.; Ihara, T.; Sugihara, S.; Takeuchi, K. *J. Mol. Catal. A* 2000, 161, 205.
- [71] Marc', G.; Augugliaro, V.; Mun'oz, M. J. L.; Martn', C.; Palmisano, L.; Rives, V.; Schiavello, M.; Tilley, R. J. D.; Venezia, A. M. *J. Phys. Chem. B* 2001, 105, 1026.
- [72] Mishra, T. *Catal. Commun.* 2008, 9, 21.
- [73] Choi, W.; Termin, A.; Hoffmann, M. R. *Angew. Chem.* 1994, 106, 1148.
- [74] Nagaveni, K.; Hegde, M. S.; Madras, G. *J. Phys. Chem. B* 2004, 108, 20204.
- [75] K. Wilke, H.D. Breuer, *J. Photochem. Photobiol. A* 121 (1999) 49.
- [76] A.G. Agrios, P. Pichat, *J. Appl. Electrochem.* 35 (2005) 655.
- [77] H. Kim, W. Choi, *Appl. Catal. B: Environ.* 69 (2007) 127.
- [78] S. Sato, J.M.White, *Chem. Phys. Lett.* 72 (1980) 83.
- [79] R. Baba, S. Nakabayashi, A. Fujishima, K. Hondas, *J. Am. Chem. Soc.* 109 (1987) 2273.
- [80] B. Ohtani, H. Osaki, S.-i. Nishimoto, T. Kagiya, *J. Am. Chem. Soc.* 108 (1986) 308.
- [81] G.N. Kryukova, G.A. Zenkovets, A.A. Shutilov, M. Wilde, K. Gu'nther, D. Fassler, K. Richter, *Appl. Catal. B: Environ.* 71 (2006) 169.
- [82] R. Asahi, T. Morikawa, T. Ohwaki, K. Aoki, Y. Taga, *Science* 293 (2001) 269.
- [83] S.G. Botta, J.A. Nav'io, M.C. Hidalgo, G.M. Restrepo, M.I. Litter, *J. Photochem. Photobiol. A* 129 (1999) 89.
- [84] H. Zou, Y.S. Lin, *Appl. Catal. A: Gen.* 265 (2004) 35.
- [85] J.L.G. Fierro, *Metal Oxides: Chemistry and Applications*, CRC press, Taylor and Francis Group, 2006, pp. 597–611.
- [86] A. Garc'ia-Ripoll, A.M. Amat, A. Arques, R. Vicente, M.F. Lo'pez, I. Oller, M.I. Maldonado, W. Gernjak, *Chemosphere* 68 (2007) 293.
- [87] D. Ljubas, *Energy* 30 (2005) 1699.
- [88] J. Aguado, R. van Grieken, M.-J. Lo'pez-Mun'oz, J. Maruga'n, *Appl. Catal. A: Gen.* 312 (2006) 202.
- [89] J. Yang, J. Zhang, L. Zhua, S. Chena, Y. Zhang, Y. Tang, Y. Zhua, Y. Li, *J. Hazard. Mater. B* 137 (2006) 952.
- [90] L. Zou, Y. Luo, M. Hooper, E. Hub, *Chem. Eng. Process.* 45 (2006) 959.

- [91] K.Y. Jung, S.B. Park, *Mater. Lett.* 58 (2004) 2897.
- [92] R.A. Doong, C.H. Chen, R.A. Maithreepala, S.M. Chang, *Water Res.* 35 (2001) 2873.
- [93] S.-L. Kuo, C.-J. Liao, *J. Chin. Chem. Soc.* 53 (2006) 1073.
- [94] W.A. Jacoby, D.M. Blake, J.A. Fennell, J.E. Boulter, L.M. Vargo, M.C. George, S.K. Dolberg, *AirWaste Manage. Assoc.* 46 (1996) 891.
- [95] T. Wang, H. Wang, P. Xu, X.C. Zhang, S. Chao, *Thin Solid Films* 334 (1998) 103.
- [96] S.E. Pratsinis, *J. Aerosol Sci.* 27 (1996) s153–s154.
- [97] Z. Ding, X. Hu, P.L. Yue, G.Q. Lu, P.F. Greenfield, *Catal. Today* 68 (2001) 173.
- [98] H.D. Nam, B.H. Lee, S. Kim, C. Jung, J. Lee, S. Park, *J. Appl. Phys.* 37 (1998) 4063.
- [99] K.Y. Jung, S.B. Park, *J. Photochem. Photobiol. A* 127 (1999) 117.
- [100] C.H.Kwon, H.Shin, J.H.Kim, W.S.Choi, K.H.Yoon, *Materials Chemistry and Physics* 86 (2004) 78-82.
- [101] S.Javed, M.Mujahid, M.Islam, U.Manzoor, *Materials Chemistry and Physics* 132 (2012) 509-514.
- [102] Zhou J, Zhang Y, Zhao X S and Ray A K, *Ind Eng Chem Res.*, 2006, 45, 3503.
- [103] Hyun-Ju Kim, Sung Bin Bae and Dong- Sik Bae, *The Azo J Mater Online*, DOI: 10.2240/azojomo0295.
- [104] Siti Aida Ibrahim, Srimala Sreekantan, *Proceedings of (ICXRI 2010) International Conference on X-Rays & Related Techniques in Research & Industry*, June 9 – 10, 2010, Aseania Resort Langkawi, Malaysia. 13669.
- [105] G. Yi, M. Sayer, *Am. Ceram. Soc. Bull.* 70 (1991) 1173.
- [106] C. Sanchez, J. Livage, M. Henry, F. Babonneau, *J. Non-Cryst. Solids* 100 (1988) 65.
- [107] G. Cao; *Nanostructures and Nanomaterials—Synthesis, Properties and Applications*; Imperial College Press, (2004).
- [108] D. P. Birnie, *Journal of Materials Science* Vol. 35, p.367 -374, (2000).
- [109] K.M.S Khalil et al., *Colloids Surfaces A. “Physicochemical Engineering Aspects*, Vol. 132 p.31-44, (1998).
- [110] D.P.Birnie, N.J.Bendzko, *Materials Chemistry and Physics*, Vol.59, p. 26-35, (1999).
- [111] A.Mills et al., *Photochemical and Photobiological Sciences*, Vol. 2, p. 591-596, (2003).
- [112] Gao, B.; Ma, Y.; Cao, Y.; Yang, W.; Yao, J. *Phys. Chem. B* 2006, 110, 14391.